

PHD THESIS

**“THE EFFECT OF ACIDIC POLYSACCHARIDES ON THE BIOGEOCHEMISTRY OF IRON
IN THE MARINE ENVIRONMENT”**

SEBASTIAN STEIGENBERGER

SUPERVISORS:

**D. WOLF-GLADROW (AWI, UNI HB), U. PASSOW (AWI), P. CROOT (IFM-
GEOMAR)**

ALFRED WEGENER INSTITUT FÜR POLAR- UND MEERESFORSCHUNG,

BREMERHAVEN

UNIVERSITÄT BREMEN

APRIL 2008

Acknowledgements

I would like to thank a number of people, who made this work possible and enjoyable during the past three years. A big thanks to my primary supervisors Uta Passow and Peter Croot, as well as to Christoph Völker und Dieter Wolf-Gladrow. Thanks also to Marta Plavsic (RBI, Croatia) and Peter Statham (NOCS, UK) for providing excellent opportunities to work at different institutes and their great collaboration. The MARMIC PhD program also offered valuable teaching opportunities and key skills training. This work was funded by the DFG and partly by the European Union under the Sixth Framework Marie Curie Actions. Special thanks also to Martha Valiadi, my friends and my family for their guidance and invaluable support.

1. Introduction	1
2. Identifying the processes controlling the distribution of H ₂ O ₂ in surface waters along a meridional transect in the Eastern Atlantic.	6
3. The role of polysaccharides and diatom exudates in the redox cycling of Fe and the photoproduction of hydrogen peroxide in coastal seawaters.	36
4. Characterization of phytoplankton exudates and polysaccharides in relation to their complexing capacity of copper, cadmium and iron.	42
5. Summary and conclusions.	80
5.1 Identifying the processes controlling the distribution of H ₂ O ₂ in surface waters along a meridional transect in the Eastern Atlantic.	81
5.2 The role of polysaccharides and diatom exudates in the redox cycling of Fe and the photoproduction of hydrogen peroxide in coastal seawaters.	81
5.3 Characterization of phytoplankton exudates and polysaccharides in relation to their complexing capacity of copper, cadmium and iron.	82
5.4 Conclusions	83
6. Future work	84
7. References	87

CHAPTER 1:

Introduction

1 Introduction

In the early 1990's the first IPCC report stated the effect of anthropogenic CO₂ emissions on global warming and John Martin's Iron Hypothesis (Martin et al. 1990), relating atmospheric Fe concentration to the CO₂ concentration in the atmosphere and the last ice age, culminating the well known sentence "Give me (half) a tanker of iron and I'll give you a new ice age!". Since then, several large scale in situ Fe fertilisation experiments revealed that in large areas of the ocean, the so called high nutrient low chlorophyll (HNLC) areas, phytoplankton growth is partly limited by depleted Fe conditions (Geider *et al.* 1994; De Baar *et al.* 2000; Boyd *et al.* 2007).

The ocean receives Fe from upwelling, deep water mixing, riverine input, melting icebergs, atmospheric dust input, input from anoxic sediments, hydrothermal vents and direct recycling by organisms. However, in HNLC regions the Fe input to surface waters is very low resulting in Fe limitation of phytoplankton growth.

Fe is an important nutrient for marine phytoplankton (Geider *et al.* 1994; Falkowski *et al.* 1998; Morel *et al.* 2003), being essential in metabolic reactions like the photosynthetic electron transport and the nitrogen assimilation. It is also required for the synthesis of chlorophyll (Martin *et al.* 1988; Maldonado *et al.* 1999) as well as for the functioning of the enzyme superoxide dismutase which inhibits the breakdown of chlorophyll by superoxide radicals (Coale 1991).

The thermodynamic stable species of Fe in oxygenated natural seawater is Fe³⁺, which undergoes rapid hydrolysis at pH 8 (Bruland *et al.* 1991). The Fe hydroxides are less soluble and precipitate finally as insoluble Fe₂O₃. Thus, Fe is continuously removed from the surface ocean via hydrolysis and scavenging after adsorption onto sinking particles(Geider 1999). Nevertheless, more than 99% of the dissolved Fe is found to be bound by organic compounds (Rue *et al.* 1995; van den Berg 1995;

Nolting *et al.* 1998; Hutchins *et al.* 1999; Croot *et al.* 2000; Boye 2001), which help retain Fe in the surface ocean. These Fe ligands comprise highly specific low molecular weight siderophores (Wilhelm *et al.* 1994; Macrellis *et al.* 2001; Butler 2005), less specific protoporphyrins (Nakabayashi *et al.* 2002), hemes (Gledhill 2007), and even less specific molecules too large for transmembrane transport (Macrellis *et al.* 2001).

Phytoplankton do not have a ligand specific uptake mechanism like prokaryotes do for siderophores. Instead eukaryotic phytoplankton take up Fe very efficiently (Voelker and Wolf-Gladrow 1999) via ferrireductase, a non specific cell surface enzyme for extracellular Fe reduction, through membrane bound transport proteins and by diffusion across plasma membrane (Croot *et al.* 1999). There are several other mechanisms to make organically bound Fe bioavailable, such as thermal dissolution (Wells *et al.* 1993), digestion by grazers (Hutchins *et al.* 1994; Barbeau *et al.* 1996) or photochemical redox processes (Waite *et al.* 1984; Sunda *et al.* 1995) using dissolved organic compounds as an electron source (Kuma *et al.* 1992).

The main oxidation pathway of Fe(II) to Fe(III) is the reaction with O₂ and H₂O₂ according to the Haber-Weiss (Millero *et al.* 1987; Millero *et al.* 1989; King *et al.* 1995). In marine systems H₂O₂ functions as a strong oxidant or a reductant (Millero *et al.* 1989; Croot *et al.* 2005). Hence, it is important for the cycling of organic compounds and trace metals like Fe (Millero *et al.* 1989). H₂O₂ is the most stable intermediate in the reduction of O₂ to H₂O and is mainly produced in the water column by photochemical reactions involving dissolved organic matter (DOM) and O₂ (Cooper *et al.* 1988; Scully *et al.* 1996; Yocis *et al.* 2000; Yuan *et al.* 2001). Light absorbed by DOM induces an electron transfer to molecular oxygen, forming the superoxide anion radical, which undergoes disproportionation to form hydrogen

peroxide. Hence light, O₂, H₂O₂ and organic compounds are important factors in the very complex chemistry of Fe in seawater. The oxidation of Fe can be inhibited (Theis *et al.* 1974; Miles *et al.* 1981) or accelerated (Sedlak *et al.* 1993; Rose *et al.* 2002, 2003) in the presence of organic compounds.

A great number of phytoplankton species release carbohydrates into the surrounding water (Myklestad *et al.* 1972; Myklestad *et al.* 1989; Myklestad 1995; Hong *et al.* 1997). Phytoplankton exudates, rich in acidic polysaccharides, account significantly for the dissolved marine organic matter pool especially during bloom events (Aluwihare *et al.* 1997; Aluwihare *et al.* 1999; Benner 2002) and are highly surface active (Mopper *et al.* 1995). These exudates and transparent exopolymer particles (TEP), abiotically formed from these exudates, show high affinity to Th and other trace elements (Santschi 1997; Quigley *et al.* 2001; Guo *et al.* 2002; Quigley *et al.* 2002).

The objective of this PhD project was to investigate the effect of acidic polysaccharides on the biogeochemistry of Fe in seawater. According to the above, three main themes were identified where research is lacking. Firstly, the specific effects of polysaccharides on Fe speciation in the light replete upper ocean were not well studied. Secondly, knowledge on the H₂O₂ distribution and influencing factors in the upper ocean is sparse despite its importance in Fe redox chemistry. Thirdly, the composition of the Fe ligand pool in the ocean was not well known. Reported chemical and biological properties of phytoplankton exudates support their Fe binding potential. The following hypotheses were made:

1.1 Polysaccharides stabilize Fe(II) via complexation

1.2 Fe bound to polysaccharides is released via photochemical processes

2. Phytoplankton exudates enhance the photoproduction of H₂O₂, a major player in the redox chemistry of Fe.

3. Acidic polysaccharides and TEP are strong Fe chelators contributing significantly to the pool of unknown organic Fe-ligands in the ocean, released by diatoms to prevent Fe from precipitating from the surface ocean

Hypotheses 1, 2 and 3 were investigated and results are presented and discussed in chapters 2, 3, and 4, respectively.

CHAPTER 2:

The role of polysaccharides and diatom exudates in
the redox cycling of Fe and the photoproduction of
hydrogen peroxide in coastal seawaters.

Sebastian Steigenberger, Peter J. Statham, Christoph
Völker and Uta Passow

(Submitted February 2008 to Marine Chemistry, manuscript number
MARCHE-S-08-00030)

The role of polysaccharides and diatom exudates in the redox cycling of Fe and the photoproduction of hydrogen peroxide in coastal seawaters

Sebastian Steigenberger¹, Peter J. Statham², Christoph Völker¹ and Uta Passow¹

¹Alfred Wegener Institut für Polar- und Meeresforschung, Am Handelshafen 12,
27570 Bremerhaven, Germany

²National Oceanography Centre, Southampton, University of Southampton Waterfront
Campus, European Way, Southampton SO14 3ZH

Abstract

The effect of artificial acidic polysaccharides (PS) and exudates of *Phaeodactylum tricornutum* on the half-life of Fe(II) in seawater was investigated in laboratory experiments. Strong photochemical hydrogen peroxide (H_2O_2) production of 5.2 to 10.9 nM (mg C)⁻¹ h⁻¹ was found in the presence of PS and diatom exudates. Furthermore when illuminated with UV light algal exudates kept the concentration of ferrous iron in seawater (initial value 100 nmol L⁻¹) elevated for about 50 min. Since no stabilising effect of PS on Fe(II) in the dark could be detected, enhanced photoreduction seems to be the cause. This was confirmed by a simple model of the photochemical redox cycle of iron. Diatom exudates seem to play an important role for the photochemistry of iron in coastal waters.

1 Introduction

Marine phytoplankton contributes significantly to the CO₂ exchange between atmosphere and ocean, thus impacting atmospheric CO₂ concentrations (Falkowski *et al.* 1998). Global marine primary productivity shows great spatial and temporal variability, caused primarily by variable light, zooplankton grazing and nutrient distributions. In addition to the macronutrients (P, N), iron is an essential trace element for photo-autotrophic organisms (Geider *et al.* 1994; Falkowski *et al.* 1998; Morel *et al.* 2003). Several large scale iron fertilization experiments have revealed that in 40% of the surface ocean, the so called High Nutrient Low Chlorophyll (HNLC) areas, iron is at least partially responsible for limitation of phytoplankton growth (Boyd *et al.* 2007). However, iron limitation can occur in coastal areas as well (Hutchins *et al.* 1998) and here the supply of Fe through upwelling and resuspension determine its cycling.

Free hydrated Fe(III) concentrations in seawater are very low (<10⁻²⁰ mol L⁻¹) (Rue *et al.* 1995) and the more soluble Fe(II) is rapidly oxidised (Millero *et al.* 1987; Millero *et al.* 1989; King *et al.* 1995; Gonzalez-Davila *et al.* 2005, 2006). Thus concentrations of dissolved Fe in the ocean should be very low. However, over 99% of the dissolved iron in seawater is reported to be bound by organic compounds (Rue *et al.* 1995; van den Berg 1995; Croot *et al.* 2000; Boye 2001) and these ligands can maintain the concentrations typically seen in the ocean (Johnson *et al.* 1997). Iron binding ligands in seawater mainly consist of bacterial siderophores (Macrellis *et al.* 2001; Butler 2005) and possibly planktonic exudates like acidic polysaccharides (PS) (Tanaka *et al.* 1971). Transparent exopolymer particles (TEP), which are rich in acidic

polysaccharides, are ubiquitous in the surface ocean (Passow 2002). TEP has been shown to bind ^{234}Th (Passow *et al.* 2006) and are therefore a prime candidate to bind iron.

The main oxidation pathway of Fe(II) to Fe(III) is the reaction with O_2 and H_2O_2 according to the Haber-Weiss mechanism (Millero *et al.* 1987; Millero *et al.* 1989; King *et al.* 1995). This oxidation can be inhibited (Theis *et al.* 1974; Miles *et al.* 1981) or accelerated (Sedlak *et al.* 1993; Rose *et al.* 2002, 2003a) in the presence of organic compounds. The decrease in apparent oxidation rate is suggested to be due to stronger photoreduction of Fe(III) (Kuma *et al.* 1995) or stabilisation of Fe(II) (Santana-Casiano *et al.* 2000; Rose *et al.* 2003b; Santana-Casiano *et al.* 2004).

In marine systems H_2O_2 functions as a strong oxidant or a reductant (Millero *et al.* 1989; Croot *et al.* 2005). Thus it is important for the cycling of organic compounds and trace metals like Fe (Millero *et al.* 1989). H_2O_2 is the most stable intermediate in the reduction of O_2 to H_2O and is mainly produced in the water column by photochemical reactions involving dissolved organic matter (DOM) and O_2 (Cooper *et al.* 1988; Scully *et al.* 1996; Yocis *et al.* 2000; Yuan *et al.* 2001). Light absorbed by DOM induces an electron transfer to molecular oxygen, forming the superoxide anion radical, which undergoes disproportionation to form hydrogen peroxide. Hence light, O_2 , H_2O_2 and organic compounds are important factors in the very complex chemistry of iron in seawater.

Increased photochemical reduction of Fe(III) in the presence of sugar acids has been reported (Kuma *et al.* 1992; Ozturk *et al.* 2004; Rijkenberg *et al.* 2005) but for polysaccharides no such studies have been carried out so far. However, the relative abundance of polysaccharides in marine dissolved organic matter (DOM) is about

50% (Benner *et al.* 1992) and in phytoplankton derived DOM the fraction of polysaccharides can be up to 64% (Hellebust 1965; Hellebust 1974). In the study reported here we investigate the effect of PS and algal exudates on the photochemical redox cycle of iron and production of H₂O₂.

2 Materials and Methods

2.1 General

Three different types of experiments were conducted to investigate the effect of PS and diatom exudates in combination with UV light on the speciation of iron and the production of H₂O₂. All experiments were conducted at a constant temperature (about 20°C) in the laboratory. In experiments 1 and 3 were samples exposed to UV radiation, UV transparent 3 L Tedlar bags were used as incubation containers. Experiment 2 was conducted in 30 mL polystyrene screw cap tubes, without UV irradiation.

The natural coastal seawater (SW) was collected in July 2006 off Lepe near Southampton (UK), filtered through 0.2 µm membranes and stored at 5°C. Organic matter was removed from a part of this SW via photo-oxidation with strong UV radiation. The so called “organic-free” UVSW (Donat *et al.* 1988) was also stored at 5°C.

We used gum xanthan, laminarin and carrageenan (all from Sigma) as the artificial PSs. The molecular weight of laminarin is 7700 g mol⁻¹ (Rice *et al.* 2004) and 43% (w/w) of the molecule is carbon. For gum xanthan and carrageenan no specifications could be found but we assumed a carbon content of ~40% (w/w).

Diatom exudates were collected as the 0.4 µm filtrate of a senescent culture of *Phaeodactylum tricornutum* grown in f/2 medium. Ford and Percival (1965) separated a significant amount of a water-soluble glucan from an aqueous extract of *Phaeodactylum tricornutum*, and their results showed this polysaccharide to be a typical chrysolaminarin with essential similar properties to the p-1,3-linked glucan, laminarin.

Philips 40TL12 and Philips 40T'05 lamps, respectively, were used as a light source for the irradiation of samples with UVB and UVA light during experiments 1 and 3. Irradiance was measured with a UVA (315-400 nm) sensor type 2.5, a UVB (280-315 nm) sensor type 1.5 (INDIUM-SENSOR, Germany) and a spherical quantum sensor SPQA 2651 (LI-COR) for the photosynthetically active radiation (PAR, 400-700 nm). Sensors were coupled to a data logger LI-1400 (LI-COR). The following irradiance values were used for all light incubations during this study: UVB=0.3 W m⁻², UVA=17.6 W m⁻² and PAR=3.8 W m⁻². For all experiments samples were held in UV transparent 3 L polyvinyl fluoride (PVF, Tedlar) bags (SKC Inc., USA), fitted with a polypropylene hose for filling and sub-sampling.

2.2 *Specific Experiments*

2.2.1 *Experiment 1: Effect of polysaccharides on the photogeneration of H₂O₂*

Four pairs of Tedlar bags were filled with MQ water and concentrated solutions of three different PSs were added to three pairs of these bags. For this experiment carrageenan, gum xanthan and laminarin were used. The PSs were dissolved in MQ water by sonicating for 30 min. The final concentration of PS was

10 mg L⁻¹ in about 2.3 L. The last pair of bags served as control and contained no PS. One bag of each pair was placed in the dark the other was illuminated with UV light for 270 min. H₂O₂ was measured 1 h before illumination and after 0, 10, 30, 90, 270 min in the light and the dark sample.

2.2.2 Experiment 2: Effect of polysaccharides on the oxidation of Fe(II) in seawater in the dark

Ten clean polystyrene screw cap tubes (30 mL) were filled with the natural Solent seawater (0.2 µm filtered) and another ten tubes were filled with the organic-free Solent Seawater. To 5 tubes of each treatment gum xanthan was added to a final concentration of 1 mg L⁻¹ and the samples were sonicated for 30 min. Initially Fe(II) equivalent to 200 nmol L⁻¹ was added to all tubes, and Fe(II) and H₂O₂ measured after 0, 2, 6, 18, 54 min. Temperature, salinity, oxygen concentration and pH were measured before the iron addition and at the end of the experiment.

2.2.3 Experiment 3: Effect of diatom exudates and UVA/B radiation on the oxidation of Fe(II) in seawater

Three Tedlar bags were filled with about 1 L of organic-free seawater (0.2 µm filtered). One bag served as a control and no further additions were made. To the second bag 100 nmol L⁻¹ Fe(II) were added. To the third bag an addition of diatom exudates and 100 nmol L⁻¹ Fe(II) was made. The amount of diatom exudates added to the sample was chosen in order to reach a concentration of PS similar to natural Solent seawater (0.4 mg glucose eq. L⁻¹). Ferrous iron concentration was measured

over a 60 min period after the iron addition. The UV light was switched on for the whole experiment right after the addition of iron to the sample bags. Temperature, salinity, oxygen concentration, pH and total iron were measured before the iron addition and at the end of the experiment. H_2O_2 in the organic-free seawater was adjusted to an initial concentration of 5 nmol L⁻¹ and was measured again at the end of the experiment.

2.3 Analyses

Iron concentrations in the samples were determined using a colorimetric method described by Stookey (1970) and Viollier *et al.* (2000). Briefly Ferrozine (the disodium salt of 3-(2-pyridyl)-5,6-bis(4-phenylsulfonic acid)-1,2,4-triazine) forms a magenta coloured tris complex with ferrous iron. The water soluble complex is stable and quantitatively formed in a few minutes at pH = 4-9 after adding an aqueous 0.01 mol L⁻¹ Ferrozine solution. The absorbance was measured with a Hitachi U-1500 at 562 nm in 10 cm cuvettes buffered with an ammonium acetate buffer adjusted to pH = 5.5, and compared to a calibration curve made by standard additions to the sample water. Standards were prepared from a 10 mmol L⁻¹ Fe(II) stock solution ($\text{Fe}(\text{NH}_4)_2(\text{SO}_4)_2 \cdot 6\text{H}_2\text{O}$ in 0.1 mol L⁻¹ HCl) diluted in 0.01 mol L⁻¹ HCl. Total iron was determined by previous reduction of the iron present in the sample under acid conditions over 2 h at room temperature by adding hydroxylamine hydrochloride (1.4 mol L⁻¹ in 5 mol L⁻¹ HCl) as the reducing agent. The detection limit of this method is about 8 nmol L⁻¹ of Fe(II) and the standard error is about 20%. All Reagents were from Sigma-Aldrich and at least p.a. grade. All solutions were prepared in MQ water (18 M Ω cm⁻¹) purified with a Millipore deionisation system.

Samples were prepared in 30 mL polystyrene screw cap tubes. All equipment has been carefully acid washed prior to use.

Concentrations of dissolved mono- and polysaccharides were determined semi quantitatively using another colorimetric method described by Myklestad *et al.* (1997). Briefly the absorbance of the strong coloured complex of 2,4,6-tripyridyl-s-triazine (TPTZ) formed with iron reduced by monosaccharides or previously hydrolyzed polysaccharides at alkaline pH is measured at 595 nm in 2.5 cm cuvettes and compared to a calibration curve prepared from D-glucose in MQ water. Total sugar concentration was determined after hydrolysis of the acidified sample in a sealed glass ampoule at 150°C for 90 min. The detection limit was 0.02 mg glucose eq. L⁻¹ and the standard error was about 3%. All glassware and reagents were prepared as described by Myklestad *et al.* (1997).

For the determination of hydrogen peroxide (H₂O₂) a chemiluminescence flow injection analysis (FIA-CL) described by Yuan and Shiller (1999) was used. The method is based on oxidation of luminol by hydrogen peroxide in an alkaline solution using Co(II) as a catalyst. Our flow injection system generally resembled that described by Yuan and Shiller (1999) but as a detection unit we used the photosensor module H8443 (Hamamatsu) with a power supply and a signal amplifier. The voltage signal was logged every second using an A/D converter and logging software (PMD-1208LS, Tracer DAQ 1.6.1.0, Measurement Computing Corporation). The chemiluminescence peaks were evaluated by calculating their area. The detection limit was 0.1 nmol L⁻¹ and the standard error was 4%. All reagents and solutions were prepared as described by Yuan and Shiller (1999). Since ferrous iron in the sample shows a significant positive interference (Yuan *et al.* 1999) H₂O₂ was measured in

parallel samples without added Fe(II) or after one hour when most of the iron was reoxidised.

A WTW 315i T/S system was used to determine temperature and salinity in the sample. Oxygen was measured using a WPA OX20 oxygen meter. The dissolved organic carbon (DOC) content in the 0.2 µm filtered samples was measured with a Shimadzu TOC-VCSN system via high temperature catalytic oxidation (HTCO) on Pt covered Al₂O₃ beads. The detection limit of this method is ~3 µmol L⁻¹ and the precision is ±2 µmol L⁻¹.

The UV photooxidation system consisted of a fan cooled 1 kW medium pressure mercury lamp (Hanovia), with 10 x 200 mL quartz tubes mounted around the axial lamp. After 6 h of UV irradiation the samples were considered “organic-free” (UVSW) (Donat *et al.* 1988). To remove the resulting high concentrations of H₂O₂ the organic-free water was treated with activated charcoal. The charcoal had previously been washed several times with HCl, ethanol and MQ water to remove contaminants. After stirring for 30-40 min the charcoal was removed by filtration through a 0.2 µm polycarbonate membrane. The H₂O₂ concentration in the resulting water was less than 0.5 nmol L⁻¹ and no contamination with iron was detectable.

3 Results and discussion

3.1 Experiment 1: Effect of polysaccharides on the photochemical production of H₂O₂

The first experiment, examining the effect of polysaccharides on the photochemical production of H₂O₂, showed that within 270 min (4.5 h) of

illumination large amounts (140-240 nmol L⁻¹) of H₂O₂ were formed due to the addition of 10 mg L⁻¹ of polysaccharides to MQ water (Figure 1). The H₂O₂ concentrations in all samples increased linearly during the experiment, after the light was switched on. Gum xanthan showed the highest photochemical production of H₂O₂ followed by carrageenan and laminarin, which can be explained by their different absorptivity at <400 nm (Figure 2). The addition of laminarin led to a net accumulation rate of H₂O₂ of 22.5 nmol L⁻¹ h⁻¹, which was twice as high as that for pure MQ water (12.3 nmol L⁻¹ h⁻¹). The H₂O₂ accumulation during illumination of the MQ water was probably due to organic matter leaching from the resin of the filter cartridge of the MQ system. However, the DOC concentration in MQ water was <<10 μmol L⁻¹. H₂O₂ accumulation rates of 36.2 nmol L⁻¹ h⁻¹ and 43.4 nmol L⁻¹ h⁻¹ were determined in samples with added carrageenan and gum xanthan, respectively. The photochemical production of H₂O₂ was thus 3-4 times higher in the presence of carrageenan and gum xanthan compared to pure MQ water. Linear H₂O₂ accumulation rates of similar magnitude have been reported by Cooper *et al.* (1988) and Miller *et al.* (1995) in natural seawater samples. The main structural differences between the molecules of these three PSs are that laminarin has a linear structure of linked glucose monosaccharide units, carrageenan has sulphur containing groups and gum xanthan has a branched structure incorporating uronic acid groups. The PS concentration used in our experiment is equivalent to about 4 mg L⁻¹ organic carbon leading to normalised H₂O₂ generation rates of 5.2 nmol L⁻¹ (mg C)⁻¹ h⁻¹ (laminarin), 9.1 nmol L⁻¹ (mg C)⁻¹ h⁻¹ (carrageenan) and 10.9 nmol L⁻¹ (mg C)⁻¹ h⁻¹ (gum xanthan). These values are up to 29 times higher than the rate of 0.38 nmol L⁻¹ (mg C)⁻¹ h⁻¹ reported by Price *et al.* (1998) for the >8000 Da fraction of natural DOM in the Western Mediterranean even though the light bulbs used in our study typically

produced only 25% of the UVB radiation 39% of UVA and 1% of PAR of the calculated natural irradiance found in midday summer sun in the Mediterranean (Zepp *et al.* 1977). The polysaccharides in our study caused strong photogeneration of H₂O₂ even under low light exposure probably due to the absence of removal processes such as enzymatic decomposition of H₂O₂ (Moffett *et al.* 1990). Photochemical production rates of H₂O₂ in the Atlantic Ocean and Antarctic waters are much lower ranging from 2.1 to 9.6 nmol L⁻¹ h⁻¹ (Obernosterer 2000; Yocis *et al.* 2000; Yuan *et al.* 2001; Gerringa *et al.* 2004). Gerringa *et al.* (2004) calculated a net production rate of 7 nmol L⁻¹ h⁻¹ at irradiance levels of 2.8 (UVB), 43 (UVA) and 346 W m⁻² (VIS/PAR) in 0.2 µm filtered water from the eastern Atlantic close to the Equator. These low rates are presumably due to lower DOC concentrations and higher decay rates due to colloids or enzymatic activity in natural waters (Moffett *et al.* 1990; Petasne *et al.* 1997). Our experiments suggest that PSs may have had a significant indirect effect on Fe oxidation due to the enhanced photochemical production of H₂O₂.

3.2 Experiment 2: Effect of gum xanthan on the oxidation of Fe(II) in the dark

Differences in the rate of Fe(II) oxidation due to added gum Xanthan were small, both in the natural SW and the UVSW samples (Figure 3 and 4). However, the oxidation of Fe(II) in the natural SW samples (with or without gum xanthan) (Figure 3) was much slower than that in the respective DOM-free UVSW samples (Figure 4). Half-life values and oxidation rates of organic-free seawater can be calculated according to Millero and Sotolongo (1989) and Millero *et al.* (1987). Under our experimental conditions the calculated half-life was 25 s for the ambient H₂O₂ concentrations and 82 s under O₂ saturation. These theoretical values can be compared

to measured Fe(II) half-life values of 42 s (UVSW) and 35 s (UVSW+PS). The measured values resemble the theoretical values under the ambient H₂O₂ conditions. This indicates that the high H₂O₂ concentration had a stronger oxidising effect on Fe(II) than the dissolved O₂ in the samples.

For the natural SW sample the theoretical half-life of 43 s under O₂ saturation does not fit the measured data well. The half-life of Fe(II) in the natural SW sample (Figure 3) was ~17 times (11.9 min) and with PS added ~19 times (13.3 min) longer than theoretical value. The measured data followed the exponential oxidation curve calculated for the low H₂O₂ concentration of these samples whereas the high O₂ content seemed to not accelerate the measured oxidation of Fe(II).

The DOC content of the natural SW (97 $\mu\text{mol L}^{-1}$) was almost 10 times higher than of the UVSW. The difference in Fe(II) oxidation between the water types might therefore be due to the stabilisation of Fe(II) against oxidation by natural occurring compounds of the coastal SW (Theis *et al.* 1974; Miles *et al.* 1981; Santana-Casiano *et al.* 2000; Rose *et al.* 2003a; Santana-Casiano *et al.* 2004). These results show that the added gum xanthan was not a good model for natural occurring substances stabilising Fe(II) against oxidation. Initial H₂O₂ concentrations also differed appreciably, with 5 nmol L^{-1} H₂O₂ in the natural SW sample and 270 nmol L^{-1} H₂O₂ in the UVSW sample. UV oxidation in UVSW water during removal of natural DOM must have caused the differences in H₂O₂. We calculated Fe(II) oxidation rates due to O₂ and H₂O₂ in our experiment to investigate if the differing rates could have been caused by differing initial H₂O₂ concentrations. From the comparison between our measured and theoretically calculated values we conclude that a strong effect of H₂O₂ on the lifetime of Fe(II) was observed but no effect of gum xanthan was found in this

experiment conducted without irradiation. The lower initial H_2O_2 concentrations in the natural SW sample ($5 \text{ nmol L}^{-1} \text{ H}_2\text{O}_2$; Figure 3) compared to the UVSW sample ($270 \text{ nmol L}^{-1} \text{ H}_2\text{O}_2$; Figure 4) appears to be the major cause for slower Fe(II) oxidation, suggesting that H_2O_2 mainly control the oxidation of Fe(II).

3.3 *Experiment 3: Effect of diatom exudates and UVA/B radiation on the oxidation of Fe(II) in seawater*

Initially, the half-lives of Fe(II) in both treatments, those with and without addition of diatom exudates, was quite similar (Figure 5). For the initial 5 min (300 s) a half life of $4.5 \pm 0.7 \text{ min}$ and $4.0 \pm 0.3 \text{ min}$, respectively was determined for Fe(II) in the UVSW without and with added diatom exudates. These values are in the same range as published values (Millero *et al.* 1987; Kuma *et al.* 1995; Croot *et al.* 2002). A remarkable difference between both treatments is clearly visible after about 7 min (420 s) (Figure 5). In the UVSW without exudates the Fe(II) concentration continued decreasing exponentially reaching the detection limit after 20 min, whereas in UVSW with added diatom exudates the Fe(II) concentration remained at about 30 nmol L^{-1} decreasing only very slightly with time. The photochemical effect of the exudates was strong enough to result in a net stabilising effect on Fe(II) after 7 minutes.

Differences in H_2O_2 production during the first hour of irradiation were significant between UVSW with and without exudates. In the UVSW sample with added diatom exudates a linear production rate of $33 \text{ nmol L}^{-1} \text{ h}^{-1} \text{ H}_2\text{O}_2$ was determined whereas in pure UVSW the respective rate was only $5 \text{ nmol L}^{-1} \text{ h}^{-1}$. The higher production rate of H_2O_2 in the presence of exudates, suggests increased photochemical production of H_2O_2 . UVSW without exudates contained $11 \mu\text{mol L}^{-1}$

DOC and no measurable total MS and PS, whereas UVSW mixed with exudates of *Phaeodactylum tricornutum* contained $\sim 450 \mu\text{mol L}^{-1}$ DOC, including 0.4 mg glucose eq. L^{-1} (i.e. $13 \mu\text{mol C L}^{-1}$) total MS and PS. The DOC- normalised H_2O_2 generation rate of $6.1 \text{ nmol L}^{-1} (\text{mg C})^{-1} \text{ h}^{-1}$ calculated from UVSW with exudates indicates that laminarin-like diatom exudates (Ford *et al.* 1965) photochemically produce H_2O_2 . However, the high DOC content suggests that there was also other organic matter contributing to the photo-production of H_2O_2 .

Figure 6 shows a schematic of that part of the iron cycle relevant for our experiment. In pure UVSW the added Fe(II) was oxidised rapidly, but in the presence of ligands contained in the diatom exudates Fe(II) formed FeL, which in the light was released as Fe(II) and then oxidised. The Fe(II) concentration could thus remain stable as Fe(II) production from FeL balanced Fe(II) oxidation. We used a simple numerical model based on these processes to model the Fe(II) concentration in our experimental system.

The model uses a constant photoproduction term $k_{\text{hv}}[\text{FeL}]$ of ferrous iron, and constant oxidation rates with oxygen (k_{O_2}). The oxidation rates with hydrogen peroxide ($k_{\text{H}_2\text{O}_2}$) are assumed to increase linearly with a photoformation rate of $33 \text{ nmol L}^{-1} \text{ h}^{-1}$ as measured in this experiment and initial H_2O_2 concentration are set at 4.6 nmol L^{-1} . The initial Fe(II) concentration $[\text{Fe(II)}_0]$ is set at 100 nmol L^{-1} Fe(II), the amount added in the experiment, and increases in the model by the constant photoreduction of the FeL complex (where L is either EDTA or diatom exudates or a combination of both). The direct photoreduction of inorganic iron colloids and dissolved ferric iron is also possible (Waite *et al.* 1984; Wells *et al.* 1991a; Wells *et al.* 1991b; Johnson *et al.* 1994), but rates for these processes are negligibly low. For

both processes together we calculated about $0.004 \text{ nmol L}^{-1} \text{ s}^{-1}$ of Fe(II) for 100 nmol L^{-1} Fe(II) added using the rates reported by Johnson et al. (1994). The model assumes that the concentration of FeL changes only negligibly during the experiment. As loss processes of Fe(II) we included the oxidation of Fe(II) with O_2 and the oxidation with H_2O_2 . The latter depends on the increasing H_2O_2 concentrations during the experiment. Since dissociation and formation of FeL are relatively slow (Hudson *et al.* 1992) compared to the photoreduction of FeL and the oxidation of Fe(II) we ignored these processes in the model. The model calculates the change in Fe(II) concentration over time (equation 1).

$$\frac{d[\text{Fe(II)}]}{dt} = k_{\text{hv}}[\text{FeL}] - k_{\text{O}_2}[\text{Fe(II)}_0] - k_{\text{H}_2\text{O}_2}[\text{H}_2\text{O}_2][\text{Fe(II)}_0] \quad \text{eq. 1}$$

$$[\text{H}_2\text{O}_2] = 33/3600 * t + 4.6 \quad \text{eq. 2}$$

t given in [s], k_{hv} and k_{O_2} in [s^{-1}], $k_{\text{H}_2\text{O}_2}$ in [$\text{L nmol}^{-1} \text{ s}^{-1}$] and all concentrations given in [nmol L^{-1}].

The parameters k_{O_2} , $k_{\text{hv}}[\text{FeL}]$ and $k_{\text{H}_2\text{O}_2}$ were estimated by fitting the model to the observed data, minimizing the root mean squared model-data misfit, scaled by the assumed variance of the measurements. If the deviations between model and data are independent and normally distributed, the misfit

$$\chi^2 = \sum_i \frac{(d_i - m_i)^2}{\sigma_i^2} \quad \text{eq. 3}$$

is a χ^2 variable. In this case we can estimate the posterior probability density function (pdf) of the model parameters (assuming a uniform prior) by

$$pdf(k_{\text{O}_2}, k_{\text{hv}}[\text{FeL}], k_{\text{H}_2\text{O}_2}) \sim \exp\left(\frac{-\chi^2}{2}\right) \quad \text{eq. 4}$$

(see e.g. D.S. Sivia (2006)). The probability function is well approximated by a multidimensional Gaussian distribution with a maximum value for the best estimated set of parameter values. To obtain an estimate of the variance for this maximum likelihood estimate of the parameters, we also need an estimate of the covariance matrix of the parameters at the minimum of χ^2 . This covariance matrix can be estimated as the inverse of the Hessian matrix of χ^2 at the minimum. We can then assume a confidence interval (\pm one standard deviation) for the best estimates of the parameters, which are $k_{O_2} = 6.04e-03 \pm 1.20e-03 \text{ s}^{-1}$, $k_{H_2O_2} = 1.97e-04 \pm 8.59e-05 \text{ L nmol}^{-1} \text{ s}^{-1}$ and $k_{hv}[FeL] = 0.22 \pm 0.06 \text{ nmol L}^{-1} \text{ s}^{-1}$. With this high photoreduction rate the model fits the measured data very well (Figure 7) but the oxidation rates for oxygen and H_2O_2 are 30% lower and 105% higher, respectively, than rates reported by Millero *et al.* (1987; 1989). Holding the oxidation rates k_{O_2} and $k_{H_2O_2}$ fixed at values calculated for the given experimental conditions (22 °C, S = 34.2, O_2 saturated, pH = 8.1) according to Millero *et al.* (1987; 1989) the model-data misfit becomes somewhat larger and the model requires a slightly higher Fe(II) photoproduction term $k_{hv}[FeL]$ of about $0.24 \pm 0.01 \text{ nmol L}^{-1} \text{ s}^{-1}$ to fit the measured data (Figure 7). The larger error margins when fitting all three parameters, compared to fitting only the photoreduction rate, is explained by the strong correlation between the estimates of $k_{H_2O_2}$ and of $k_{hv}[FeL]$, meaning that the data can be represented almost equally well with different combinations of these two parameters.

The estimated photoproduction rates of Fe(II) are about 50 times higher than the photoreduction rate of inorganic colloidal and dissolved iron calculated before, independent of whether we assume the oxidation rates by Millero *et al.* (1987, 1989). This indicates high photoreduction of Fe(III) mediated by the added organic material. This high reduction of Fe(III) could have resulted either from direct photoreduction of

the FeL or indirectly via light induced (see absorbance spectra Figure 2) formation of superoxide ($\text{DOM} + h\nu \rightarrow \text{DOM}^*$; $\text{DOM}^* + \text{O}_2 \rightarrow \text{DOM}^+ + \text{O}_2^-$; and $\text{Fe(III)} + \text{O}_2^- \rightarrow \text{Fe(II)} + \text{O}_2$) and the subsequent reduction of ferric iron (King *et al.* 1995; Voelker *et al.* 1995; Rose *et al.* 2005; Fujii *et al.* 2006; Rose *et al.* 2006; Waite *et al.* 2006; Garg *et al.* 2007b, 2007a).

Since the estimated laminarin concentration of $\sim 1 \text{ mg L}^{-1}$ only accounts for $\sim 8\%$ of the DOC content of this sample it is not clear to what extend PS were responsible for the photoreduction during this experiment. Some EDTA (concentration of $\sim 1 \mu\text{mol L}^{-1}$) had inadvertently also been added with the diatom exudates, as it was part of the culture media. However, photoreduction of iron from complexes with EDTA seemed to have had only a minor effect. Reported steady state Fe(II) concentrations present under stronger irradiation due to photoreduction of Fe-EDTA complexes are much lower (Sunda *et al.* 2003) than observed in this study. Photo-redox cycling of Fe-EDTA complexes has a larger influence on Fe(III) concentrations than on those of Fe(II) (Sunda *et al.* 2003).

Steady state concentrations of photochemical Fe(II) are linearly related to the irradiation energy especially in the UV range (Kuma *et al.* 1995; Rijkenberg *et al.* 2005; Rijkenberg *et al.* 2006; Laglera *et al.* 2007). In our study the light intensity was only 25% of the UVB radiation 39% of UVA and 1% of PAR of the calculated natural irradiance in midday summer sun at 40°N (Zepp *et al.* 1977). Therefore under natural coastal conditions, with 4-5 times lower DOC concentrations but a 2.6 to 100 times higher irradiance levels, a photoreductive effect of diatom exudates seems highly probable.

4 Conclusions

In this study we investigated the photochemical effect of artificial and natural polysaccharide material in aquatic systems on iron speciation and on the production of H₂O₂. Artificial PS caused high photochemical production of H₂O₂, which acts as a strong oxidant for metals and organic matter on the one hand. On the other hand H₂O₂ is formed photochemically via the superoxide intermediate which is capable of reducing Fe(III). We found increased steady state Fe(II) concentrations in illuminated seawater with a high concentration of exudates of *Phaeodactylum tricornutum*. In the dark this effect of artificial PS on ferrous iron was not detectable, suggesting that light-produced superoxide reduces Fe(III) maintaining elevated Fe(II) concentration. In coastal seawater with high content of organic matter originating partly from diatoms a positive effect of the exudates on the bioavailability of iron seems likely. Field studies comparing natural phytoplankton bloom waters with open ocean waters are needed to confirm these photoreduction results and the counteracting effect of H₂O₂ on a daily time scale and as a function of particle size (dissolved, colloidal and particulate fraction).

5 Acknowledgments

We thank P. Goody for his help in the laboratory at the NOCS (UK) and T. Steinhoff and S. Grobe who measured the DOC in our samples at the IfM-Geomar (Germany). Thanks also to N. McArdle for administrative help during this BIOTRACS Early-Stage Training (EST) Fellowship which was funded by the European Union under the Sixth Framework Marie Curie Actions.

6 References

- Benner, R., J. D. Pakulski, *et al.* (1992). "Bulk chemical characteristics of dissolved organic matter in the ocean." *Science* **255**: 1561-1564.
- Boyd, P. W., T. Jickells, *et al.* (2007). "Mesoscale iron enrichment experiments 1993–2005: synthesis and future directions." *Science* **315**: 612-617.
- Boye, M. (2001). "Organic complexation of iron in the Southern Ocean." *Deep Sea Research I* **48**(6): 1477-1497.
- Butler, A. (2005). "Marine Siderophores and Microbial Iron Mobilization." *BioMetals* **18**(4): 369-374.
- Cooper, W. J., R. G. Zika, *et al.* (1988). "Photochemical formation of H₂O₂ in natural waters exposed to sunlight." *Environ. Sci. Technol.* **22**: 1156-1160.
- Croot, P. L. and M. Johansson (2000). "Determination of iron speciation by cathodic stripping voltammetry in seawater using the competing ligand 2-(2-Thiazolylazo)-p-cresol (TAC)." *Electroanalysis* **12**(8): 565-576.
- Croot, P. L. and P. Laan (2002). "Continuous shipboard determination of Fe(II) in polar waters using flow injection analysis with chemiluminescence detection." *Analytica Chimica Acta* **466**: 261-273.
- Croot, P. L., P. Laan, *et al.* (2005). "Spatial and temporal distribution of Fe(II) and H₂O₂ during EisenEx, an open ocean mesoscale iron enrichment." *Mar. Chem.* **95**: 65-88.
- Donat, J. R. and K. W. Bruland (1988). "Direct determination of dissolved Cobalt and Nickel in seawater by differential pulse cathodic stripping voltammetry preceded by adsorptive collection of cyclohexane-1,2-dione dioxime complexes." *Anal. Chem.* **60**: 240-244.
- Falkowski, P. G., R. T. Barber, *et al.* (1998). "Biogeochemical controls and feedbacks on ocean primary production." *Science* **281**(5374): 200-206.
- Ford, C. W. and E. Percival (1965). "The carbohydrates of *Phaeodactylum tricornutum*." *J. Chem. Soc.*: 7035-7041.
- Fujii, M., A. L. Rose, *et al.* (2006). "Superoxide-mediated dissolution of amorphous ferric oxyhydroxide in seawater." *Environmental Science & Technology* **40**(3): 880-887.
- Garg, S., A. L. Rose, *et al.* (2007a). "Superoxide-mediated reduction of organically complexed iron(III): Impact of pH and competing cations (Ca²⁺)."*Geochimica Et Cosmochimica Acta* **71**: 5620-5634.

Garg, S., A. L. Rose, *et al.* (2007b). "Superoxide mediated reduction of organically complexed Iron(III): Comparison of non-dissociative and dissociative reduction pathways." *Environmental Science & Technology* **41**(9): 3205-3212.

Geider, R.J., *et al.* (1994). "The role of iron in phytoplankton photosynthesis and the potential for iron-limitation of primary productivity in the sea." *Photosynth. Res.* **39**: 275-301.

Gerringa, L. J. A., M. J. A. Rijkenberg, *et al.* (2004). "The influence of solar ultraviolet radiation on the photochemical production of H₂O₂ in the equatorial Atlantic Ocean." *J. Sea Res.* **51**: 3-10.

Gonzalez-Davila, M., J. M. Santana-Casiano, *et al.* (2005). "Oxidation of iron (II) nanomolar with H₂O₂ in seawater." *Geochimica et Cosmochimica Acta* **69**(1): 83-93.

Gonzalez-Davila, M., J. M. Santana-Casiano, *et al.* (2006). "Competition between O₂ and H₂O₂ in the oxidation of Fe(II) in natural waters." *Journal of Solution Chemistry* **35**(1): 95-111.

Hellebust, J. A. (1965). "Excretion of some organic compounds by marine phytoplankton." *Limnol. Oceanogr.* **10**: 192-206.

Hellebust, J. A. (1974). "Extracellular products. In: W. D. P. Stewart, (Ed.), Algal physiology and biochemistry." *Blackwell*: 838-863.

Hudson, R.J.M, *et al.* (1992). "Investigations of iron coordination and redox reactions in seawater using ⁵⁹Fe radiometry and ion-pair solvent extraction of amphiphilic iron complexes." *Marine Chemistry* **38**: 209-235.

Hutchins, D. A. and K. W. Bruland (1998). "Iron-limited diatom growth and Si:N uptake ratios in a coastal upwelling regime." *Nature* **393**: 561-564.

Johnson, K. S., K. H. Coale, *et al.* (1994). "Iron photochemistry in seawater from the equatorial Pacific." *Mar. Chem.* **46**: 319-334.

Johnson, K. S., R. M. Gordon, *et al.* (1997). "What controls dissolved iron concentrations in the world ocean?" *Marine Chemistry* **57**(3 / 4): 137.

King, D. W., H. A. Lounsbury, *et al.* (1995). "Rates and mechanism of Fe(II) oxidation at nanomolar total iron concentrations." *Environ. Sci. Technol.* **29**: 818-824.

Kuma, K., S. Nakabayashi, *et al.* (1995). "Photoreduction of Fe(III) by hydrocarboxylic acids in seawater." *Water Research* **29**(6): 1559-1569.

Kuma, K., S. Nakabayashi, *et al.* (1992). "Photoreduction of Fe(III) by dissolved organic substances and existence of Fe(II) in seawater during spring blooms." *Mar. Chem.* **37**: 15-27.

Laglera, L. M. and C. M. G. Van den Berg (2007). "Wavelength dependence of the photochemical reduction of iron in arctic seawater." *Environ. Sci. Technol.* **41**: 2296-2302.

Macrellis, H. M., C. G. Trick, *et al.* (2001). "Collection and detection of natural iron-binding ligands from seawater." *Marine Chemistry* **76**: 175-187.

Miles, C. J. and P. L. Brezonik (1981). "Oxygen consumption in humic-colored waters by a photochemical ferrous-ferric catalytic cycle." *Environ. Sci. Technol.* **15**(9): 1089-1095.

Miller, W. L., D. W. King, *et al.* (1995). "Photochemical redox cycling of iron in coastal seawater." *Mar. Chem.* **50**: 63-77.

Millero, F. J. and S. Sotolongo (1989). "The oxidation of Fe(II) with H₂O₂ in seawater." *Geochim. Cosmochim. Acta* **53**: 1867-1873.

Millero, F. J., S. Sotolongo, *et al.* (1987). "The oxidation kinetics of Fe(II) in seawater." *Geochim. Cosmochim. Acta* **51**: 793-801.

Moffett, J. W. and O. C. Zafiriou (1990). "An investigation of hydrogen peroxide in surface waters of Vineyard Sound with H₂¹⁸O₂ and ¹⁸O₂." *Limnol. Oceanogr.* **35**: 1221-1229.

Morel, F. M. M. and N. M. Price (2003). "The biogeochemical cycles of trace metals in the oceans." *Science* **300**: 944-947.

Myklestad, S. M., E. Skanoy, *et al.* (1997). "A sensitive and rapid method for analysis of dissolved mono- and polysaccharides in seawater." *Marine Chemistry* **56**(3-4): 279-286.

Obernosterer, I. B. (2000). "Photochemical transformations of dissolved organic matter and its subsequent utilization by marine bacterioplankton." *PhD thesis*: 133 pp.

Ozturk, M., P. L. Croot, *et al.* (2004). "Iron enrichment and photoreduction of iron under UV and PAR in the presence of hydroxycarboxylic acid: implications for phytoplankton growth in the Southern Ocean." *Deep Sea Research II* **51**: 2841-2856.

Passow, U. (2002). "Transparent exopolymer particles (TEP) in aquatic environments." *Progress in Oceanography* **55**: 287-333.

Passow, U., J. Dunne, *et al.* (2006). "Organic carbon to ²³⁴Th ratios of marine organic matter." *Mar. Chem.* **100**: 323-336.

Petasne, R. G. and R. G. Zika (1997). "Hydrogen peroxide lifetimes in south Florida coastal and offshore waters." *Mar. Chem.* **56**: 215-225.

Price, D., R. F. C. Mantoura, *et al.* (1998). "Shipboard determination of hydrogen peroxide in the western Mediterranean sea using flow injection with chemiluminescence detection." *Analytica Chimica Acta* **377**: 145-155.

Rice, P. J., B. E. Lockhart, *et al.* (2004). "Pharmacokinetics of fungal (1-3)- β -Image-glucans following intravenous administration in rats." International Immunopharmacology **4**(9): 1209-1215.

Rijkenberg, M. J. A., A. C. Fischer, *et al.* (2005). "The influence of UV irradiation on photoreduction of iron in the Southern Ocean." Mar. Chem. **93**: 119-129.

Rijkenberg, M. J. A., L. J. A. Gerringa, *et al.* (2006). "Enhancement and inhibition of iron photoreduction by individual ligands in open ocean seawater." Geochimica Et Cosmochimica Acta **70**(11): 2790-2805.

Rose, A. L. and D. Waite (2006). "Role of superoxide in the photochemical reduction of iron in seawater." Geochimica Et Cosmochimica Acta **70**(15): 3869-3882.

Rose, A. L. and T. D. Waite (2002). "Kinetic model for Fe(II) oxidation in seawater in the absence and presence of natural organic matter." Environ. Sci. Technol. **36**: 433-444.

Rose, A. L. and T. D. Waite (2003a). "Effect of Dissolved Natural Organic Matter on the Kinetics of Ferrous Iron Oxygenation in Seawater." Environ. Sci. Technol. **37**: 4877-4886.

Rose, A. L. and T. D. Waite (2003b). "Kinetics of iron complexation by dissolved natural organic matter in coastal waters." Marine Chemistry **84**(1-2): 85-103.

Rose, A. L. and T. D. Waite (2005). "Reduction of organically complexed ferric iron by superoxide in a simulated natural water." Environmental Science & Technology **39**(8): 2645-2650.

Rue, E. L. and K. W. Bruland (1995). "Complexation of iron(III) by natural organic ligands in the central North Pacific as determined by a new competitive ligand equilibrium / adsorptive cathodic stripping voltammetric method." Marine Chemistry **50**: 117-138.

Santana-Casiano, J., M. G.-D. Vila, *et al.* (2000). "The effect of organic compounds in the oxidation kinetics of Fe(II)." Marine Chemistry **70**(1-3): 211-222.

Santana-Casiano, J. M., M. Gonzalez-Davila, *et al.* (2004). "The oxidation of Fe(II) in NaCl-HCO₃- and seawater solutions in the presence of phthalate and salicylate ions: a kinetic model." Mar. Chem. **85**(1-2): 27-40.

Scully, N. M., D. J. McQueen, *et al.* (1996). "Hydrogen peroxide formation: The interaction of ultraviolet radiation and dissolved organic carbon in lake waters along a 43-75 degrees N gradient." Limnol. Oceanogr. **41**(3): 540-548.

Sedlak, D. L. and J. Hoigne (1993). "The role of copper and oxalate in the redox cycling of iron in atmospheric waters." Atmospheric Environment **27A**(14): 2173-2185.

- Sivia, D. S. (2006). "Data Analysis, A Bayesian Tutorial." 246 pp.
- Stookey, L. L. (1970). "Ferrozine - a new spectrophotometric reagent for iron." Anal. Chem. **42**(7): 779-781.
- Sunda, W. and S. Huntsman (2003). "Effect of pH, light, and temperature on Fe-EDTA chelation and Fe hydrolysis in seawater." Mar. Chem. **84**: 35-47.
- Tanaka, Hurlburt, *et al.* (1971). "Application of Algal Polysaccharides as *in vivo* Binders of Metal Pollutants." Proceedings of the International Seaweed Symposium **7**: 602-604.
- Theis, T. L. and P. C. Singer (1974). "Complexation of Iron(II) by organic matter and its effect on Iron(II) oxygenation." Environ. Sci. Technol. **8**: 569-573.
- van den Berg, C. M. G. (1995). "Evidence for organic complexation of iron in seawater." Marine Chemistry **50**: 139-157.
- Viollier, E., P. W. Inglett, *et al.* (2000). "The ferrozine method revisited: Fe(II)/Fe(III) determination in natural waters." Applied Geochemistry **15**(6): 785-790.
- Voelker, B. M. and D. L. Sedlak (1995). "Iron reduction by photoproduced superoxide in seawater." Mar. Chem. **50**: 93-102.
- Waite, T. D. and F. M. M. Morel (1984). "Photoreductive dissolution of colloidal iron oxides in natural waters." Environmental Science & Technology **18**: 860-868.
- Waite, T. D., A. L. Rose, *et al.* (2006). "Superoxide-mediated reduction of ferric iron in natural aquatic systems." Geochimica Et Cosmochimica Acta **70**(18): A681-A681.
- Wells and M. L. a. L.M.~Mayer (1991a). "The photoconversion of colloidal iron oxyhydroxides in seawater." Deep-Sea-Research A **38**: 1379-1395.
- Wells, M., L. Mayer, *et al.* (1991b). "The photolysis of colloidal iron in the oceans." Nature **252**: 248-250.
- Yocis, B. H., D. J. Kieber, *et al.* (2000). "Photochemical production of hydrogen peroxide in Antarctic Waters." Deep Sea Research I **47**(6): 1077-1099.
- Yuan, J. and A. M. Shiller (1999). "Determination of subnanomolar levels of hydrogen peroxide in seawater by reagent-injection chemiluminescence detection." Analytical Chemistry **71**(10): 1975-1980.
- Yuan, J. and A. M. Shiller (2001). "The distribution of hydrogen peroxide in the southern and central Atlantic ocean." Deep Sea Research II **48**: 2947-2970.
- Zepp, R. G. and D. M. Cline (1977). "Rates of direct photolysis in aquatic environment." Environ. Sci. Technol. **11**(4): 359-366.

7 Figures

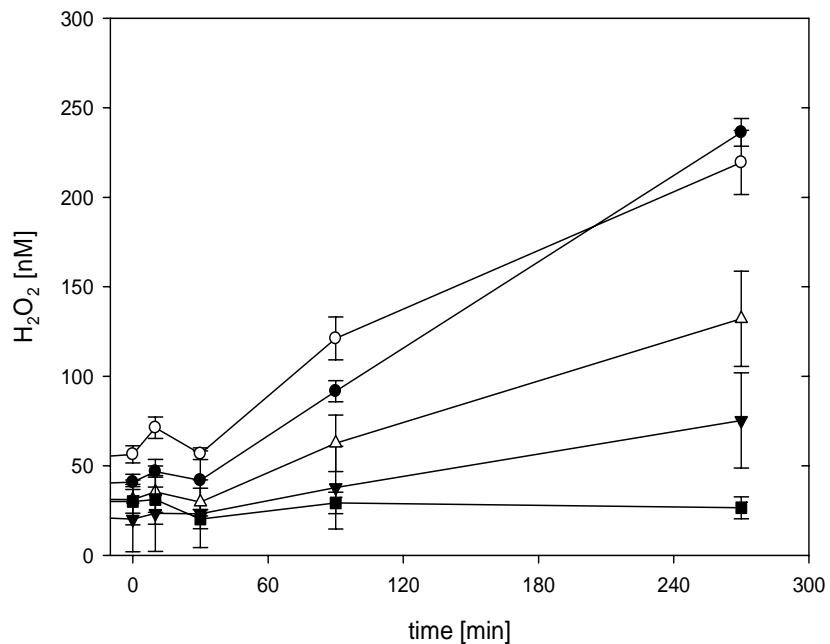


Figure 1: Photogeneration of H_2O_2 during 270 min of irradiation of a 10 mg L^{-1} solution of laminarin (open triangle), carrageenan (open circle), gum xanthan (filled circle) and of pure MQ water (filled triangle) and the mean of all 4 dark controls (filled squares)

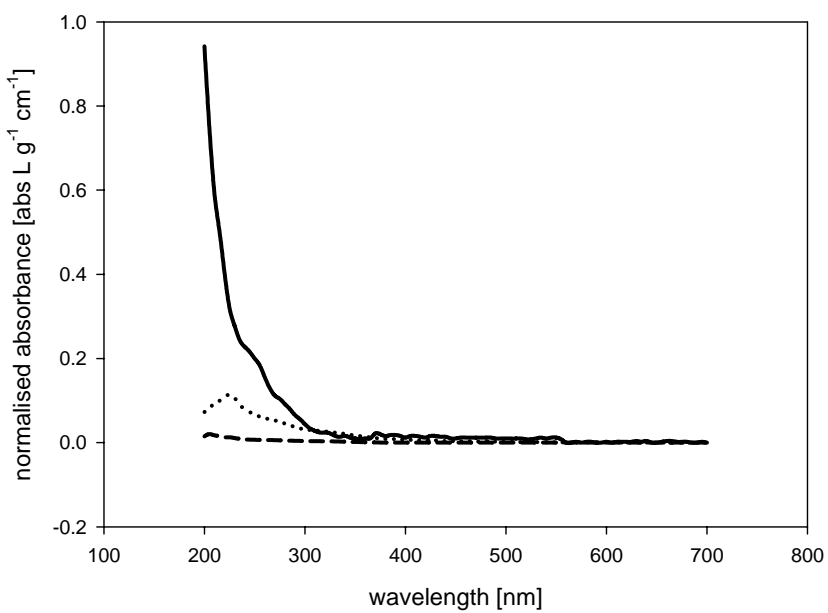


Figure 2: Absorbance spectra (normalised absorbance for 1 g L^{-1} and 5 cm cuvette) of laminarin (dashed line), carrageenan (dotted line), gum xanthan (solid line) dissolved in MQ water and filtered over $0.2 \mu\text{m}$ membrane

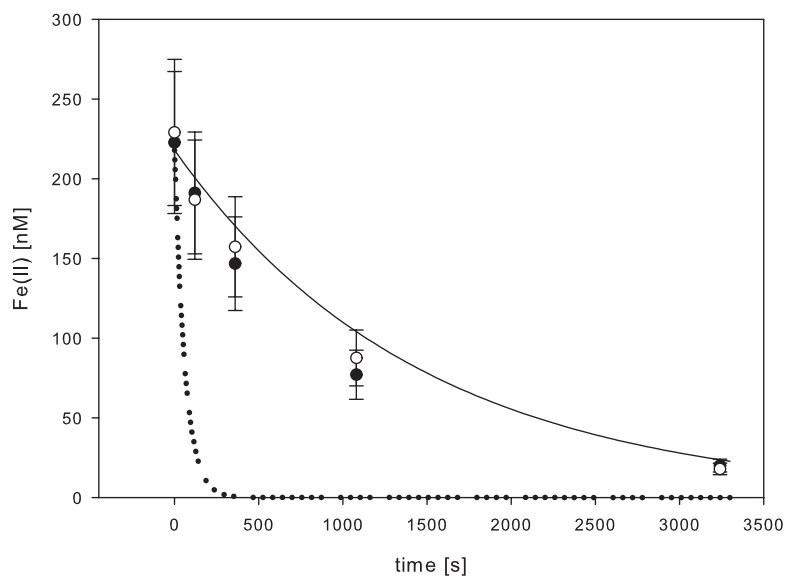


Figure 3: Dark oxidation of 218 nmol L^{-1} Fe(II) in natural SW (filled circles) and natural SW with PS added. Model results of oxidation of Fe (II) under O_2 saturation (dotted line) and in the presence of 5 nmol L^{-1} H_2O_2 (solid line) at $\text{pH} = 8.4$, $S = 34.1$, 18°C are also depicted

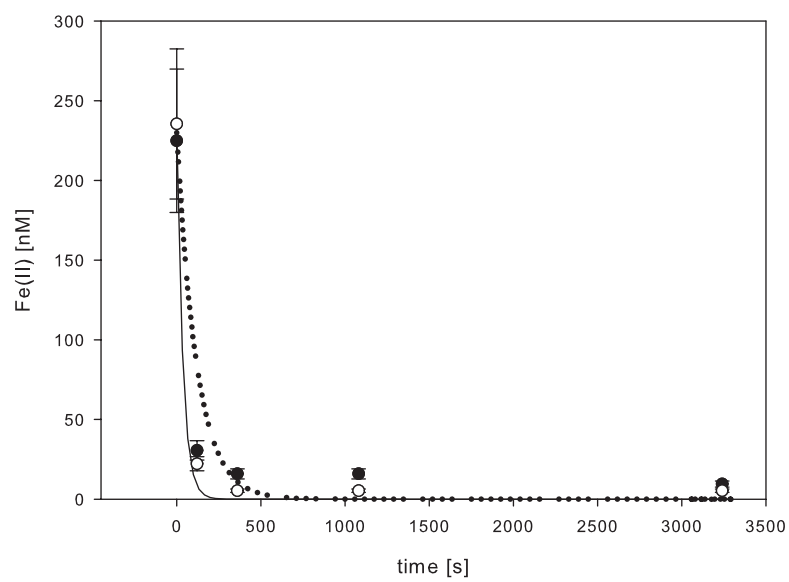


Figure 4: Dark oxidation of 230 nmol L^{-1} Fe(II) in UVSW (filled circles) and UVSW with PS added. Model results of oxidation of Fe (II) under O_2 saturation (dotted line) and in the presence of 270 nmol L^{-1} H_2O_2 (solid line) at $\text{pH} = 8.3$, $S = 34.1$, 17°C are also depicted

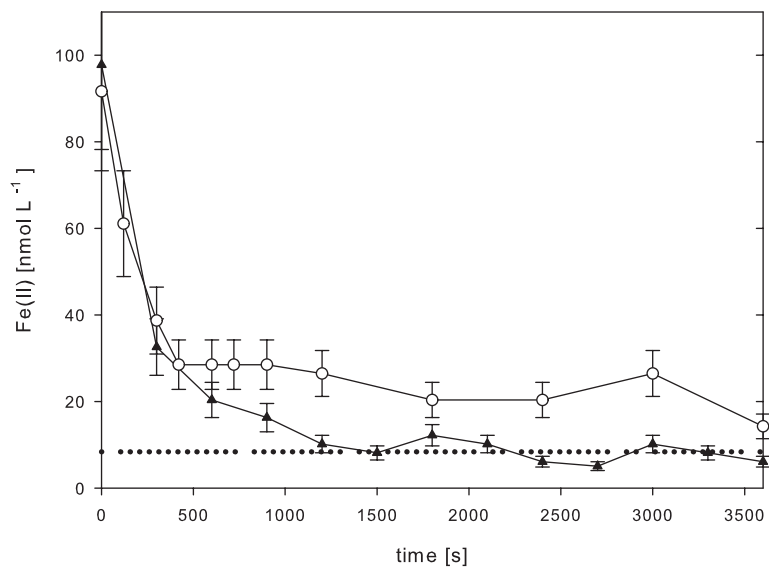


Figure 5: Oxidation of Fe(II) in pure UVSW (triangles) and in UVSW with added diatom exudates (circles) ($22\text{ }^{\circ}\text{C}$, $S = 34.2$, O_2 saturated, $\text{pH} = 8.1$, $\text{UVB} = 0.3 \text{ W m}^{-2}$, $\text{UVA} = 17.6 \text{ W m}^{-2}$, $\text{PAR} = 3.8 \text{ W m}^{-2}$). The dotted line depicts the detection limit.

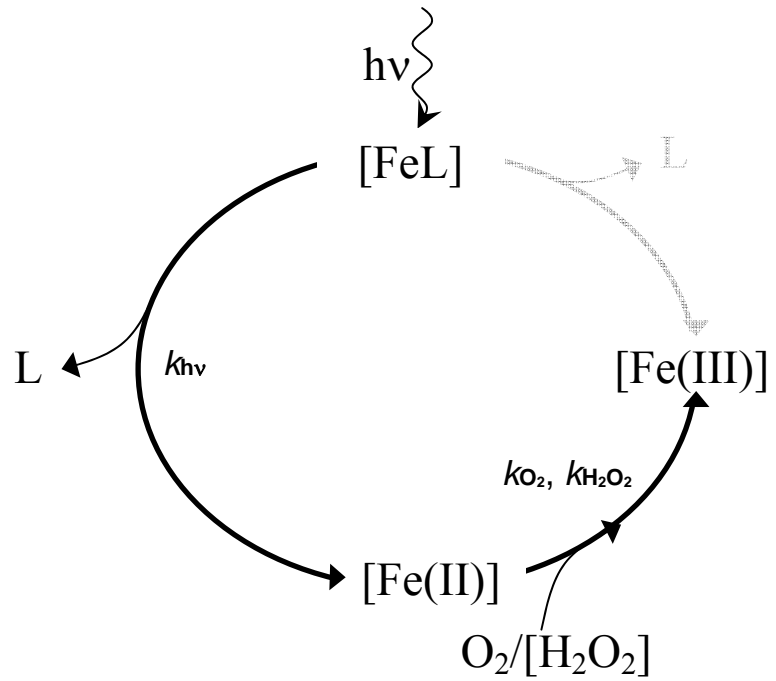


Figure 6: Schematic photoredox cycle for FeL describing the Fe cycling in experiment 3 adapted from Sunda and Huntsman (2003)

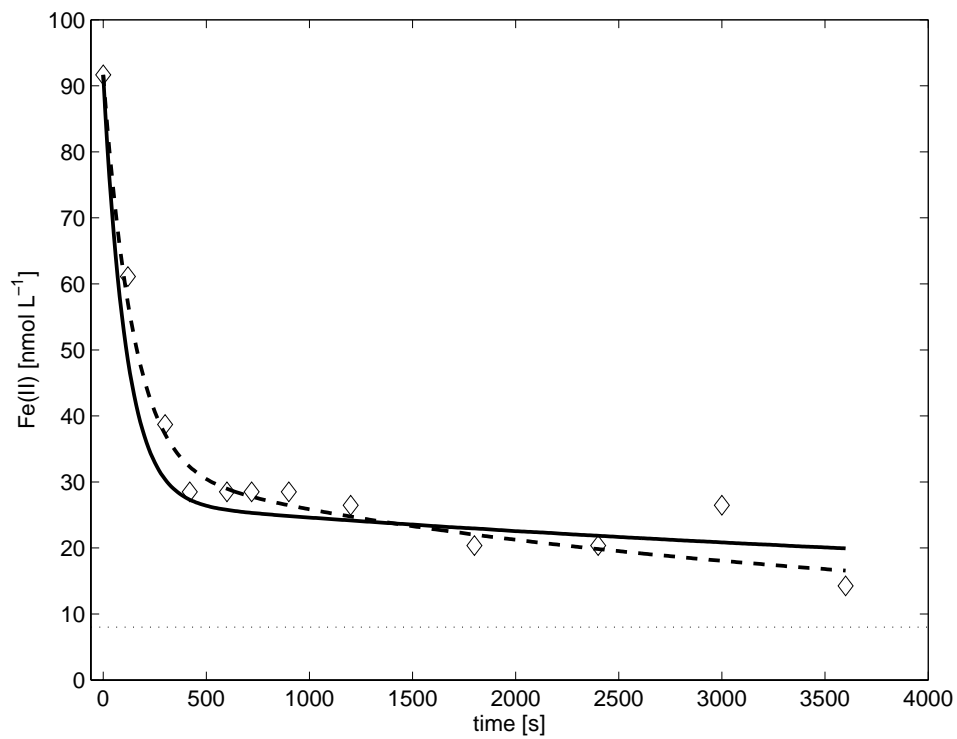


Figure 7: Best curve fits for measured data (experiment 3) of the oxidation of Fe(II) in UVSW (22 °C, pH = 8.1) with added diatom exudates (diamonds) using fix oxidation rates calculated according to Millero *et al.* (1987; 1989) and the best estimate for the photoproduction term (solid line) and using the best parameter estimates for all three parameters (dashed line) the dotted line shows the detection limit

CHAPTER 3:

Identifying the processes controlling the
distribution of H₂O₂ in surface
waters along a meridional transect in the eastern
Atlantic.

Sebastian Steigenberger and Peter L. Croot

(Steigenberger and Croot (2008) Identifying the processes controlling the distribution of H₂O₂ in surface waters along a meridional transect in the eastern Atlantic. Geophys. Res. Lett. 35, L03616,
doi:10.1029/2007GL032555)

Identifying the processes controlling the distribution of H₂O₂ in surface waters along a meridional transect in the eastern Atlantic

S. Steigenberger¹ and P. L. Croot²

Received 7 November 2007; revised 17 December 2007; accepted 7 January 2008; published 13 February 2008.

[1] Hydrogen peroxide (H₂O₂) is an important oxidant for many bio-relevant trace metals and organic compounds and has potential as a tracer for mixing in near surface waters. In this study we combine H₂O₂ and bio-optical measurements with satellite data for a meridional transect from 46°N to 26°S in the eastern Atlantic in order to determine the key processes affecting its distribution. Surface H₂O₂ ranged from 21–123 nmol L⁻¹, with maximum inventories (0–200 m) of 5.5–5.9 mmol m⁻² found at 30°N and 25°S. Analyses showed a strong positive correlation of surface H₂O₂ with daily irradiances and recent precipitation, though poor correlations with CDOM suggest sunlight is the limiting reactant for H₂O₂ formation. Vertical distributions of H₂O₂ were controlled by a combination of mixing processes and phytoplankton activity. The present study highlights processes controlling global H₂O₂ distributions and points towards the development of parameterization schemes for prediction via satellite data. **Citation:** Steigenberger, S., and P. L. Croot (2008), Identifying the processes controlling the distribution of H₂O₂ in surface waters along a meridional transect in the eastern Atlantic, *Geophys. Res. Lett.*, 35, L03616, doi:10.1029/2007GL032555.

1. Introduction

[2] In marine systems H₂O₂ functions as a strong oxidant or a reductant and thus it is important for the cycling of organic compounds and trace metals like Fe [Millero and Sotolongo, 1989]. H₂O₂ is the most stable intermediate in the four-electron reduction of O₂ to H₂O and is mainly produced in the water column by photochemical reactions involving dissolved organic matter (DOM) and O₂ [Yuan and Shiller, 2001]. Light absorbed by DOM induces an electron transfer to O₂ forming O₂^{·-}, which undergoes disproportionation to form H₂O₂. Typical open ocean H₂O₂ profiles show an exponential decrease from a surface maximum consistent with the downwelling irradiance. Maximum concentrations of 300 nmol L⁻¹ have been reported in Equatorial and Tropical regions with high DOM concentrations as for the Amazon plume [Croot et al., 2004]. In regions with low DOM and low sunlight, surface H₂O₂ levels are much lower with Southern Ocean values of 10–20 nmol L⁻¹ [Croot et al., 2005].

[3] Another potential source for H₂O₂ in surface seawater is from precipitation which preferentially removes H₂O₂

from the atmosphere during rain events [Cohan et al., 1999], consequently the atmospheric input at the equator and in the Inter Tropical Convergence Zone (ITCZ) is high [Croot et al., 2004; Weller and Schrems, 1993; Yuan and Shiller, 2000] compared to areas with less precipitation. H₂O₂ in the ocean is also produced biologically by phytoplankton [Palenik and Morel, 1988]. While photochemical production is considered the dominant pathway for H₂O₂ formation, in a few cases in the Southern Ocean, distinct H₂O₂ maximum at depth, corresponding to the chlorophyll maximum, suggest a significant biological source of H₂O₂ [Croot et al., 2005].

[4] Removal pathways also determine H₂O₂ concentrations in the water column and include the Catalase and Peroxidase activity of phytoplankton [Moffett and Zafiriou, 1990] along with redox reactions with reduced metals (e.g. Fe(II) and Cu(II)) [Millero and Sotolongo, 1989; Moffett and Zika, 1987]. The ‘dark decay life-time’ of H₂O₂ can vary from hours to weeks in the ocean [Petasne and Zika, 1997], but typically is around 4 days in the open ocean [Plane et al., 1987]. Overall, the decay rate of H₂O₂ is apparently controlled by several factors including H₂O₂ concentration, colloid concentration, bacteria/cyanobacteria numbers and temperature, which controls enzymatic decay [Wong et al., 2003; Yuan and Shiller, 2001]. Due to its short lifetime H₂O₂ shows potential as a tracer for recent vertical mixing activity [Johnson et al., 1989].

[5] In the present study we compare H₂O₂ profiles with physical and bio-optical measurements and available satellite data to determine the major processes controlling the distribution of H₂O₂ in the upper ocean along a meridional transect in the eastern Atlantic.

2. Methods

2.1. Sampling

[6] Samples were collected during the GEOTRACES cruise, ANTXXIII-I from 14 October to 17 November 2005 on board the German research vessel *R. V. Polarstern* on a transect between Bremerhaven and Cape Town. Six to seven depths were sampled for H₂O₂ from the upper 200 m at 19 stations (Figure 1), at local noon, using Niskin bottles on a standard CTD rosette. All analytical work was carried out in an AirClean class 100 laminar flow clean bench. Chlorophyll and chromophoric dissolved organic matter (CDOM) were measured in samples collected from the same CTD/rosette cast.

[7] By sampling only at local noon we were unable to examine the importance of the solar driven diel cycle in H₂O₂, by which variations of up to 40 nmol L⁻¹ H₂O₂ have been reported with maxima in the afternoon or early evening [Yuan and Shiller, 2001; Zika et al., 1985a; Zika

¹Alfred-Wegener-Institut für Polar- und Meeresforschung, Bremerhaven, Germany.

²FB2 Marine Biogeochemistry, Leibniz-Institut für Meeresswissenschaften (IFM-Geomar), Kiel, Germany.

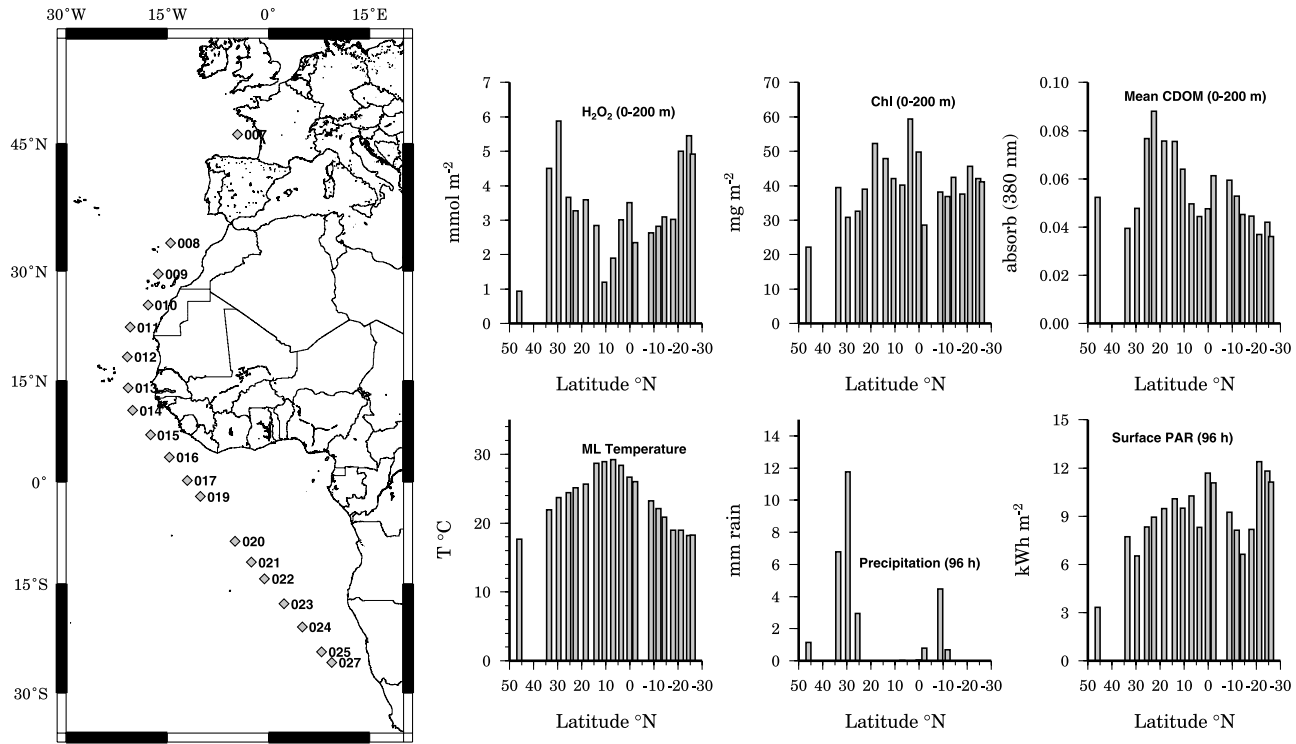


Figure 1. (left) ANTXXIII-1 cruise transect with location of the sampling stations. (right) Representative latitudinal distributions of some of the analysed parameters along the ANTXXIII-1 cruise transect. Clockwise from top left: H₂O₂ inventory (0–200 m), chlorophyll inventory (0–200 m), mean CDOM in the upper 200 m, surface PAR for the preceding 96 hours (source: HelioClim-2 database), precipitation for the preceding 96 hours (source: TRMM data), and mixed layer temperature.

et al., 1985b]. In the present work by sampling at the local noon, we are able to provide a valid comparison between stations along the transect but it is clear more work on the diel cycling of H₂O₂ is required.

2.2. H₂O₂ Measurements in Surface Waters

[8] Samples were drawn into 100 mL low density brown polyethylene bottles which were impervious to light. Unfiltered samples for H₂O₂ were analyzed within 1–2 h of collection using a flow injection chemiluminescence (FIA-CL) reagent injection method [Yuan and Shiller, 1999] as described by Croot *et al.* [2004]. Five replicates of each sample were analyzed with a typical precision of 2–3% in the concentration range of 2–120 nmol L⁻¹ and a detection limit (3σ) of typically 0.6 nmol L⁻¹.

2.3. Measurement of the Natural Light Field Within the Upper Water Column

[9] A freefalling spectroradiometer (SPMR, Satlantic) was deployed for measuring the natural light field within the upper water column (down to 150–200 m). The spectral downwelling irradiance was measured at 13 wavelengths covering a spectral range from 339–682 nm.

2.4. Photosynthetically Active Radiation (PAR) Data

[10] Hourly sub-surface PAR (400–700 nm) estimates for the sampling period were obtained from the HelioClim-2 database (http://www.soda-is.com/eng/services/service_invoke/gui.php) which is constructed from METEOSAT data using the Heliosat-2 method [Rigollier *et al.*, 2004].

2.5. Measurement of Chlorophyll and CDOM Within the Upper Water Column

[11] The samples were filtered to collect the particulate matter and then stored in liquid nitrogen. Samples were analyzed post-cruise with HPLC (High Performance Liquid Chromatography) by R. A. Reynolds and D. Stramski (Scripps Institution of Oceanography, U.S.). Spectral absorption measurements of CDOM at 326 and 380 nm were made onboard the ship by R. Röttgers (GKSS Research Centre, Germany) using PSICAM [Röttgers and Doerffer, 2007].

2.6. Other Parameters

[12] Salinity, temperature and transmission were measured via a CTD (SBE 911plus, Sea-Bird Electronics). The integrated (over 3 h) precipitation data in mm were obtained from NASA TRMM (Tropical Rainfall Measuring Mission) product 3B42 using the GIOVANNI web-interface (<http://daac.gsfc.nasa.gov/techlab/giovanni/>).

2.7. Statistics

[13] A Spearman rank test was performed on the data which yielded pairwise correlation coefficients (ρ) between the parameters. All statistical analyses were done with SigmaStat 3.1 (Systat Software Inc.).

3. Results

3.1. Latitudinal Patterns of H₂O₂, Irradiance, SST, Chlorophyll/CDOM, and Precipitation During ANT XXIII-1

[14] A transect from 46°N to 26°S across the Atlantic covers a wide range of upper ocean environments [Sarthou

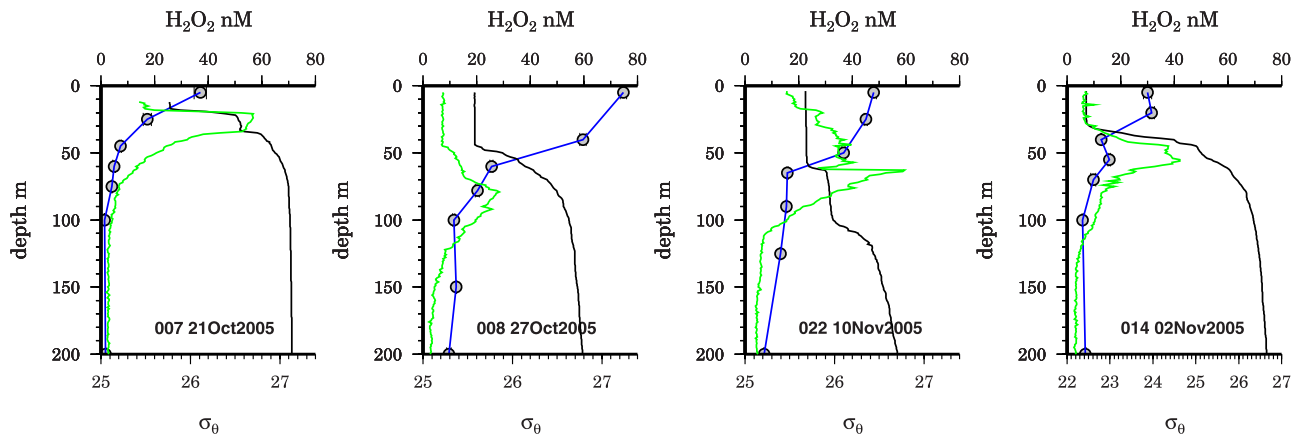


Figure 2. Vertical profiles of H₂O₂ (black circles on blue line), density σ_θ (black line), and chlorophyll fluorescence (green line, arbitrary fluorescence units where the x-axis spans from 0 to 1) showing (left) the characteristic exponential decrease (representing Stn PS 69/007, 10–13, 15–20, 24–27), (middle left) the effect of 7 mm precipitation (previous 96 h accumulated, PS 69/008), (middle right) the effect of vertical mixing (representing Stn 21–23), and (right) coinciding peaks in chlorophyll fluorescence and H₂O₂ (representing Stn 9, 14).

et al., 2003]. Surface chlorophyll concentrations ranged from 0.09–0.29 $\mu\text{g L}^{-1}$, the sea surface temperature (SST) ranged from 18–29°C with H₂O₂ inventories (0–100 m) ranging from 0.9–5.9 mmol m^{-2} (Figure 1). Highest H₂O₂ inventories between 5.5–5.9 mmol m^{-2} were found at stations 009 (30°N) and 025 (24°S), consistent with the earlier findings of Yuan and Shiller [2005], lowest inventories of 0.9–1.29 mmol m^{-2} at stations 007 (46°N) and 014 (10°N) (Figure 1). The highest integrated (0–200 m) chlorophyll values of 50–60 mg m^{-2} were found off Mauritania (Stn PS 69/012) and near the Equator (Stn 016) (Figure 1). CDOM absorbance, averaged over 0–200 m depth, was highest off north–west Africa (Stn 010–014) (Figure 1).

[15] Both the measured instantaneous PAR and the temperature of the mixed layer (Figure 1) reached maximum values near the Equator at station 016 and 15 respectively and decreased until station 021. Significant precipitation events (5–12 mm) occurring in the preceding 4 days before station occupation were detected for the stations off Morocco (Stn 008–009) and in the South Atlantic (Stn 021) (Figure 1).

3.2. Vertical Distribution of H₂O₂, Light, and Chlorophyll/CDOM During ANT XXIII-1

[16] The vertical profiles of H₂O₂ show the typical exponential decrease in the upper 50–100 m (Figure 2). At most of the stations H₂O₂ concentrations below 100 m depth were <10 nmol L^{-1} . Lowest surface concentrations (<30 nmol L^{-1}) were found in the Bay of Biscay (Stn PS 69/007) and at station 014 (10°N) coinciding with cloudy conditions. Maximum concentrations (123 nmol L^{-1}) were recorded in the southern Angola Basin (Stn 025) under clear skies. The vertical distribution of H₂O₂ in the Angola Basin (i.e. Stn PS 69/021–023) showed a deviation from the expected exponentially decrease, with almost constant H₂O₂ concentrations for the upper 50 m, followed by a strong decrease towards 60–80 m (Figure 2). At stations 009 and 014 small increases in H₂O₂ concentrations anom-

alous from the normal exponential pattern coincided with both the chlorophyll and CDOM maxima.

[17] Surface chlorophyll was elevated in the Bay of Biscay (Stn 007), off Mauritania (Stn 012), and in the Angola Basin (Stn 023). Vertical chlorophyll profiles showed subsurface maxima and sharp decreases with depth. Maximum surface absorbance of CDOM at 380 nm was observed in the Bay of Biscay (Stn 007) and off Mauritania (Stn 012). CDOM absorbance was low at the surface and reached highest values at the chlorophyll maximum and stayed high until 200 m depth. The average euphotic depth (1% PAR, z_{eu}) was 70 m (range 45–101 m) along the transect.

3.3. Statistical Analyses

[18] See Table 1. The vertical distribution of H₂O₂ was strongly correlated, as expected, with irradiance and was strongest at 442 nm ($\rho = 0.86$ $p < 0.05$ $df = 56$) and to a lesser extent with both PAR and UVA (340 nm). The vertical distribution of CDOM and H₂O₂ revealed a modest negative correlation ($\rho = -0.57$ $p < 0.05$ $df = 72$). H₂O₂ and chlorophyll depth distributions in turn were weakly correlated ($\rho = 0.32$ $p < 0.05$ $df = 75$). The depth of the chlorophyll maximum and the depth of maximum CDOM absorbance correlated strongly ($\rho = 0.76$ $p < 0.05$ $df = 15$, Stn 021–023 excluded due to strong mixing in the upper water column). A further strong correlation existed between vertical profiles of H₂O₂ and temperature ($\rho = 0.75$ $p < 0.05$ $df = 131$).

[19] A modest negative correlation was calculated for H₂O₂ inventories over the MLD and the average temperature over the MLD ($\rho = -0.56$ $p < 0.05$ $df = 18$), which becomes very strong ($\rho = -0.96$ $p < 0.05$ $df = 11$) excluding the stations of significant precipitation (Stn 7–10, 19–21). Strongly negative correlated were surface H₂O₂ concentrations and surface chlorophyll concentrations ($\rho = -0.75$ to -0.92). Modest and strong correlations ($\rho = 0.66$ and -0.74) were found between PAR and UVA irradiation respectively and surface H₂O₂ concentrations. Precipitation

Table 1. Results of Spearman Rank Analysis of Correlations Between H₂O₂ and Potentially Important Parameters^a

	Irradiance			Water Temperature	Chlorophyll, HPLC	CDOM, absorbance at 380 nm	Precipitation $\geq 1\text{ mm}$
	PAR	340 nm	442 nm				
H₂O₂ Surface Data							
$\rho = \dots$	0.28(0.66)	0.40(0.74)	0.29(0.48)	-0.22 (-0.44)	-0.75 (-0.92)	-0.28 (-0.11)	0.86
$p = \dots$	0.25(<0.05)	0.08(< 0.05)	0.22(0.11)	0.37 (0.14)	<0.05(<0.05)	0.24 (0.72)	<0.05
df = ...	18(II)	18(II)	18(II)	18 (11)	18 (11)	18 (11)	6
H₂O₂ Inventories							
—	—	—	—	-0.56(-0.96) ^b $< 0.05(<\mathbf{0.05})$	0.20 (0.01) ^c 0.4 (0.96)	-0.38 (-0.40) ^d 0.11(0.19)	—
—	—	—	—	18 (11)	18 (II)	18 (11)	—
H₂O₂ Depth profiles							
0.71 (0.72)	0.72(0.72)	0.83(0.86)	0.75 (0.65)	0.32 (0.25)	-0.57 (-0.52)	—	—
<0.05 (<0.05)	<0.05(<0.05)	<0.05(<0.05)	<0.05 (<0.05)	<0.05 (<0.05)	<0.05 (0.09)	<0.05 (<0.05)	—
63 (40)	69 (42)	84(56)	131 (82)	75 (47)	72 (47)	72 (47)	—

^aCorrelations measured are surface concentrations, water column inventories, and discrete concentrations at depth. Values in brackets were determined excluding stations of significant precipitation (Stn 7–10, 19–21).

^bTemperature averaged over MLD, H₂O₂ integrated over MLD.

^cIntegrated over 0–200 m.

^dCDOM absorbance averaged over 0–200 m, H₂O₂ integrated over 0–200 m.

and surface H₂O₂ values correlated strongly ($\rho = 0.86$ $p < 0.05$ df = 6) at the seven stations affected by rain. Excluding stations of significant rainfall generally increased the strength of the correlations in the surface data.

[20] Estimated noon sub-surface PAR values from the HelioClim-2 database were in good agreement with the measured instantaneous PAR ($\rho = 0.70$ $p < 0.05$ df = 18). Excluding the stations of significant precipitation (Stn 7–10 and 19–21) the sub-surface PAR estimates integrated over 24, 48 and 96 h before sampling correlated modestly with surface H₂O₂ ($\rho = 0.66$ –0.84 $p < 0.05$ df = 11).

4. Discussion

[21] Our results show that the distribution and inventories of H₂O₂ observed during ANT XXIII-1 were affected by several factors related to variations in the sources, sinks and physical mixing at each location. H₂O₂ inventories were strongly negatively correlated to the SST in line with expected temperature effects on enzymatic sinks for H₂O₂ [Wong *et al.*, 2003]. Inventories of H₂O₂ decreased equatorwards in contrast to SST and daily PAR irradiance (Figure 1). The highest observed H₂O₂ inventories (0–100 m) were found at the start and near the end of the cruise (Figure 1) possibly reflecting a balance between photo-formation and temperature-dependent loss processes. The strong negative relationship between H₂O₂ and chlorophyll at the surface is probably related to increased Catalase and Peroxidase activity arising from increased phytoplankton biomass [Moffett and Zafiriou, 1990]. Latitudinal decreases in H₂O₂ suggest that sink terms are more sensitive to temperature than the photo-formation of H₂O₂ is to irradiance, a finding consistent with recent studies in the North–West Pacific [Yuan and Shiller, 2005]. Inventories of H₂O₂ decreased by 49% from station PS 69/009 to 016 despite an increase in irradiance of 49% (Figure 1), this may arise from the simultaneous increase in SST by 25% (Figure 1). However, there is a strong correlation of surface H₂O₂ and UV irradiance (340 nm) underlining the importance of UV radiation for the photo-formation of H₂O₂ [Gerringa *et al.*, 2004]. The modest to strong positive correlation of surface H₂O₂ with the preceding 24, 48 and 96 h total sub-surface PAR flux indicates that, away from areas of precipitation,

there is a clear connection to the “light history” at each station. Since instantaneous irradiation data can not solely explain distribution patterns of H₂O₂ in seawater, databases such as HelioClim-2 are a useful new tool for estimating the “light history” in the Ocean.

[22] The vertical distribution of H₂O₂ was dominated by irradiance (Table 1) with most stations showing a characteristic exponential decrease (Figure 2). The correspondence of the chlorophyll and CDOM maximum with the local increases in H₂O₂ 009 and 014 (Figure 2) suggest either; production of H₂O₂ by phytoplankton [Croot *et al.*, 2005; Palenik and Morel, 1988] or from fresh photo-labile phytoplankton exudates. Station 014 (Figure 2) shows the inverse shape of the depth profiles of CDOM and H₂O₂ causing the modest negative correlation between these parameters (Table 1) which is related to photobleaching of CDOM in surface waters [O’Sullivan *et al.*, 2005].

[23] At Station 008, high surface H₂O₂ levels show the effect of precipitation (Figures 1 and 2) on H₂O₂ levels. Although the number of rain events was small they correlated strongly with H₂O₂ surface concentrations (Table 1) confirming that rain is an important source for H₂O₂ to the surface ocean [Croot *et al.*, 2004]. In the Angola Basin (Stn 021–23), strong mixing in the upper water column with the euphotic depth (z_{eu}) and the MLD roughly equivalent, resulted in significantly higher H₂O₂ concentrations at depth than at other locations (Figure 2), highlighting the importance of upper ocean mixing processes [Johnson *et al.*, 1989] on H₂O₂ distribution. It should be noted however that strong mixing has no apparent effect on H₂O₂ inventories. The strong correlation between vertical profiles of temperature and H₂O₂ (Table 1) is not unexpected as both parameters are forced by sunlight and have similar vertical distributions, in our study region, with highest values at the surface and decreasing values with depth. Increased temperatures should shorten the lifetime of H₂O₂ [Moffett and Zika, 1987; Wong *et al.*, 2003] which is seen in the negative correlation between H₂O₂ inventories and SST.

5. Conclusion

[24] Measurements of H₂O₂ during ANT XXIII-1 show a number of factors influenced its distribution. The latitudinal

patterns observed indicate irradiance, water temperature and recent precipitation as key controls. Vertical distributions of H₂O₂ were strongly controlled by photo-formation and mixing processes in the upper water column. The recent irradiation history and phytoplankton activity appear to be the key sources and sinks in determining the observed H₂O₂ levels, with CDOM playing a minor role suggesting sunlight is the key limiting reactant in the formation of H₂O₂ in the Tropical and Sub-Tropical surface ocean. This work points to the future possibilities of developing satellite based estimations of H₂O₂ in the global ocean.

[25] **Acknowledgments.** The authors would like to show their deep thanks and appreciation to the crew of the R.V. Polarstern, for all their efforts in helping us throughout ANTXXIII-1. Thanks also to the Chief Scientist, Michiel Rutgers van der Loeff, and to the AWI for making this cruise possible. Thanks to D. Stramski, R. A. Reynolds, M. Stramska, S. Kaczmarek, R. Röttgers, K. Heymann and A. Ruser for providing the irradiance, chlorophyll and CDOM data. This manuscript was greatly improved by Uta Passow and two anonymous reviewers. The work was also partly financed by a Deutsche Forschungsgemeinschaft (DFG) project awarded to PLC (CR145/7-1) and by the DFG Excellence Cluster, "The Future Ocean". This work is also a contribution to the German SOLAS (SOPRAN) program.

References

- Cohan, D. S., M. G. Schultz, D. J. Jacob, B. G. Heikes, and D. R. Blake (1999), Convective injection and photochemical decay of peroxides in the tropical upper troposphere: Methyl iodide as a tracer of marine convection, *J. Geophys. Res.*, **104**, 5717–5724.
- Croot, P. L., P. Streu, I. Peeken, K. Lochte, and A. R. Baker (2004), Influence of the ITCZ on H₂O₂ in near surface waters in the equatorial Atlantic Ocean, *Geophys. Res. Lett.*, **31**, L23S04, doi:10.1029/2004GL020154.
- Croot, P. L., et al. (2005), Spatial and temporal distribution of Fe (II) and H₂O₂ during EISENEX, an open ocean mesoscale iron enrichment, *Mar. Chem.*, **95**, 65–88.
- Gerringa, L. J. A., et al. (2004), The influence of solar ultraviolet radiation on the photochemical production of H₂O₂ in the equatorial Atlantic Ocean, *J. Sea Res.*, **51**, 3–10.
- Johnson, K. S., et al. (1989), Hydrogen peroxide in the western Mediterranean Sea: A tracer for vertical advection, *Deep Sea Res.*, **26**, 241–254.
- Millero, F. J., and S. Sotolongo (1989), The oxidation of Fe (II) with H₂O₂ in seawater, *Geochim. Cosmochim. Acta*, **53**, 1867–1873.
- Moffett, J. W., and O. C. Zafiriou (1990), An investigation of hydrogen peroxide in surface waters of Vineyard Sound with H₂¹⁸O₂ and ¹⁸O₂, *Limnol. Oceanogr.*, **35**, 1221–1229.
- Moffett, J. W., and R. G. Zika (1987), Reaction kinetics of hydrogen peroxide with copper and iron in seawater, *Environ. Sci. Technol.*, **21**, 804–810.
- O'Sullivan, D. W., et al. (2005), Photochemical production of hydrogen peroxide and methylhydroperoxide in coastal waters, *Mar. Chem.*, **97**, 14–33.
- Palenik, B., and F. M. M. Morel (1988), Dark production of H₂O₂ in the Sargasso Sea, *Limnol. Oceanogr.*, **33**, 1606–1611.
- Petasne, R. G., and R. G. Zika (1997), Hydrogen peroxide lifetimes in south Florida coastal and offshore waters, *Mar. Chem.*, **56**, 215–225.
- Plane, J. M. C., et al. (1987), Photochemical modeling applied to natural waters, in *Photochemistry of Environmental Aquatic Systems*, edited by R. G. Zika and W. J. Cooper, pp. 215–224, Am. Chem. Soc., Washington, D. C.
- Rigollier, C., et al. (2004), The method Heliosat-2 for deriving shortwave solar radiation from satellite images, *Sol. Energy*, **77**, 159–169.
- Rottgers, R., and R. Doerffer (2007), Measurements of optical absorption by chromophoric dissolved organic matter using a point-source integrating-cavity absorption meter, *Limnol. Oceanogr. Methods*, **5**, 126–135.
- Sarthou, G., et al. (2003), Atmospheric iron deposition and sea-surface dissolved iron concentrations in the East Atlantic, *Deep Sea Res., Part I*, **50**, 1339–1352.
- Weller, R., and O. Schrems (1993), H₂O₂ in the marine troposphere and seawater of the Atlantic Ocean, *Geophys. Res. Lett.*, **20**, 125–128.
- Wong, G. T. F., et al. (2003), The decomposition of hydrogen peroxide by marine phytoplankton, *Oceanol. Acta*, **26**, 191–198.
- Yuan, J., and A. M. Shiller (1999), Determination of subnanomolar levels of hydrogen peroxide in seawater by reagent-injection chemiluminescence detection, *Anal. Chem.*, **71**, 1975–1980.
- Yuan, J. C., and A. M. Shiller (2000), The variation of hydrogen peroxide in rainwater over the South and Central Atlantic Ocean, *Atmos. Environ.*, **34**, 3973–3980.
- Yuan, J., and A. M. Shiller (2001), The distribution of hydrogen peroxide in the southern and central Atlantic ocean, *Deep Sea Res., Part II*, **48**, 2947–2970.
- Yuan, J., and A. M. Shiller (2005), Distribution of hydrogen peroxide in the northwest Pacific Ocean, *Geochem. Geophys. Geosyst.*, **6**, Q09M02, doi:10.1029/2004GC000908.
- Zika, R. G., et al. (1985a), Spatial and temporal variations of hydrogen peroxide in Gulf of Mexico waters, *Geochim. Cosmochim. Acta*, **49**, 1173–1184.
- Zika, R. G., et al. (1985b), Hydrogen peroxide concentrations in the Peru Upwelling area, *Mar. Chem.*, **17**, 265–275.

P. L. Croot, FB2 Marine Biogeochemie, Leibniz-Institut für Meereswissenschaften (IFM-Geomar), Dienstgebäude Westufer, Düsternbrooker Weg 20, D-24105 Kiel, Germany. (pcroot@ifm-geomar.de)

S. Steigenberger, Alfred-Wegener-Institut für Polar- und Meeresforschung, Am Handelshafen 12, D-27570 Bremerhaven, Germany.

CHAPTER 4:

Characterization of phytoplankton exudates and
phytagel in relation to their complexing capacity of
copper, cadmium and iron

Slađana Strmečki¹, Marta Plavšić¹ Sebastian

Steigenberger and Uta Passow²

(Manuscript in preparation for submission to Marine Chemistry)

**Characterization of phytoplankton exudates and phytogel in relation to their
complexing capacity of copper, cadmium and iron**

Sladana Strmečki¹, Marta Plavšić¹, Sebastian Steigenberger^{2,3}, Uta Passow^{2,4}

¹Ruđer Bošković Institute, Center for Marine and Environ. Res. Zagreb, PO Box 180, 10002 Zagreb, Croatia

² Alfred Wegener Institute for Polar and Marine Research, Bremerhaven, Am Handelshafen 12 , D-27570 Germany

³ presently: National Oceanography Centre, Southampton, University of Southampton, European Way, Waterfront Campus, Southampton, SO14 3ZH, UK

⁴ presently: Marine Science Institute, University of California Santa Barbara, CA 93106

Abstract

The goals of this study were to determine electrochemically, the complexing capacity of organic matter released by cultures of two marine diatoms *Thalassiosira weissflogii* and *Skeletonema costatum*, as well as the coccolithophore *Emiliania huxleyi* to copper (CCu) and cadmium (CCd) as well as to determine the organic matter responsible for the complexation. In particular, the constituents of organic matter whose effects were investigated were reduced sulphur species (RSS), of surface active substances (SAS) and thio/amino groups. These measurements were combined with colorimetric analyses of transparent exopolymer particles (TEP) and carbohydrates to investigate their role in the complexation of Cu and Cd. Phytigel, carrageenan, laminarin and alginic acid were analysed as model substances, where the former was analyzed for complexation of Cu and Cd and the three latter for complexation of iron. In these experiments, solutions of polysaccharides were titrated with the relevant trace metal in order to determine the apparent stability constant of the resulting complexes.

The organic matter released by all three phytoplankton cultures and the polysaccharide phytigel complexed Cu and to a lesser extent Cd. However, Cd complexes showed higher apparent stability constants and consequently the exudates and phytigel bound Cd more specifically than Cu. Sulphur-rich “glutathione” type ligands were found in all phytoplankton samples and were possibly responsible for the complexation of Cu. The correlation of monosaccharides with the complexing capacity to Cd, indicated that in the phytoplankton samples these compounds bound Cd. TEP, SAS and polysaccharides did not appear to be primarily responsible for the complexing properties of the phytoplankton samples. No specific iron binding properties of laminarin, carrageenan, phytigel and alginic acid could be found probably partly due to limitations of the applied electrochemical methods. However, these measurements confirmed that the analysed model polysaccharides are highly surface active.

INTRODUCTION

Phytoplankton contribute quantitatively and in terms of reactivity significantly to the pool of dissolved organic matter in the ocean (Benner et al. 1992, Aluwihare et al. 1997, Aluwihare & Repeta 1999, Benner 2002). A significant fraction of marine organic matter acts as ligands for trace metals. In surface waters > 99% of copper (Cu), cadmium (Cd), or iron (Fe) for example exist complexed to organic ligands (Bruland, 1992; Buck and Bruland, 2005; Buckley and van den Berg, 1986). Phytoplankton have the capability of producing such metal complexing ligands (Bruland et al., 1991), and consequently phytoplankton composition and activity may control trace metal speciation, e.g. (Muller et al., 2003). However, ligands that bind different metals differ physico-chemically, and temporal and spatial variability of the speciation of any one metal is also high, e.g. (Blake et al., 2004). Due to this complexity, the chemical structure of metal binding ligands remains largely unknown. However, different substance classes, including sulfur rich substances like thiols, surface active substances (SAS), transparent exopolymer particles (TEP) and polysaccharides are thought to be of major importance as potential ligands.

Sulfur-groups have a very strong affinity to most heavy metals and the sulfur metal complex is very stable. Sulfur containing compounds, like glutathione (a tripeptide) and other thiols are important ligands found in phytoplankton cultures and in natural seawater (Leal et al., 1999; Laglera and van den Berg, 2003; Laglera and van den Berg, 2006; Dryden et al., 2006). Glutathione has been shown to be an especially important compound of the ligands responsible for the nearly complete complexation of Cu in seawater (Ross et al., 2003).

SAS include a variety of organic substances (proteins, polysaccharides, humic type substances) which possess hydrophobic (e.g. fatty acids chains, aromatic rings, hydrocarbons) and hydrophilic functional groups (e.g. NH₂, COOH, OH, SH) and therefore participate in electrostatic and hydrophobic interactions (Ćosović, 2005). SAS act as metal ligands and bind

Cu well (Plavšić et al., 2006). Operationally defined, SAS accumulate at phase boundaries e.g. in nature at the seawater – atmosphere or particle surface – seawater boundary (Liss and Duce, 1997). Thus SAS that act as ligand concentrate the respective trace metal on surfaces, determining the partitioning of the trace metal.

Specific polysaccharides common in the ocean, e.g. alginic acid or carrageenans have been shown to bind metal ions (Gimenez et al., 1995; Kim et al., 1995). Acidic PS and especially S-rich PS, rather than the more abundant neutral ones are thought to be primarily responsible for the binding of trace elements (Santschi et al. 2006). TEP are rich in acidic polysaccharides (uronic acids or PS with sulfated or phosphorelated acidic groups) that make them extremely surface active (Mopper et al. 1995, Zhou et al. 1998). Specifically the high affinity of acidic PS to thorium and trace metals like iron, have been shown (Honeyman & Santschi 1991, Quigley et al. 2002, Passow et al. 2006). By binding trace elements (Quigley et al. 2001, Guo et al. 2002), both as TEP and as dissolved TEP-precursors that form TEP abiotically (Passow 2000), the PS determine the biochemical cycling of these trace substances (Verdugo et al. 2004, Santschi et al., 2006, Scoullos et al., 2006) and their bioavailability.

Nevertheless, our knowledge of phytoplankton derived ligands for trace elements is scarce, partially because of the high complexity, and partially because these type of investigations are methodologically challenging.

Electrochemical methods allow the determination of the complexing capacity of trace metal ions, as well as the characterization of organic matter possibly responsible for binding trace metals. Such methods include: 1) a titration that determines the complexing capacity for Cu and Cd ions in natural seawater using the static mercury drop electrode (SMDE)(Plavšić et al 1982 ; Plavšić, 2003; Scoullos et al., 2004; Plavšić et al., 2006) ; 2) the constant current potentiometric analysis (CPSA), which detects amino- and/or thio- groups (Ciglenečki et al. 2000; Ciglenečki et al. 2003); 3) a voltammetric method to determine the concentration of

reduced sulfur species (RSS) (Ciglenečki and Čosović, 1996) and 4) a voltammetric method to determine the concentration and type of surface active substances (SAS) adsorbed on the mercury electrode (Čosović, 1985; Kozarac et al. 1989; Plavšić et al., 1990). 5) The iron binding strength of the model substances phytigel, carrageenan, laminarin and alginic acid was investigated using competitive ligand exchange cathodic stripping voltammetry (CLE-CSV) as described by Croot et al. (2002). 6) Square wave voltammetry (SWV) scans were performed, to identify Fe complexes of carrageenan, laminarin and alginic acid. Colorimetric methods measuring concentrations of transparent exopolymer particles (TEP) and carbohydrates (polysaccharide and monosaccharide) provide a different approach to characterizing marine organic matter potentially important for binding of trace metals. Electrochemical and colorimetrical methods characterizing marine organic matter, have never been really compared, except in the paper dealing with a mucilage event in the coastal sea (Scoullos et. al. 2006) in which similar approach was applied.

The goal of this study was to characterize the complexing capacity of organic matter released by phytoplankton to copper (Cu) and cadmium (Cd) and characterize the organic matter responsible for the complexation. The above mentioned electrochemical methods are combined with colorimetrical analysis of transparent exopolymer particles (TEP) and carbohydrates released by phytoplankton to investigate if TEP, carbohydrates, reduced sulfur species (RSS), thio/amino groups (CPSA) and surface active substances (SAS) play a central role for the complexing of Cu and Cd. The complexing capacity for copper and cadmium was investigated in three marine phytoplankton cultures, two diatoms (*Bacillariophyceae*), *Thalassiosira weissflogii* and *Skeletonema costatum*, as well as the coccolithophore (*Prasynophyceae*) *Emiliania huxleyi*. Organic matter in all three cultures was characterized in parallel and related to the complexing capacity. Phytigel was used as a model substance. The complexing properties of several polysaccharides (PS) - alginic acid (g mol^{-1}), laminarin,

carrageenan (sulphurous polysaccharide)– were investigated using the square wave voltammetry (SWV) and competitive ligand exchange cathodic stripping voltammetry (CLE-CSV).

MATERIALS AND METHODS

The complexing capacities of the organic material to copper and cadmium (Co, Cd) were determined in the three cultures and three size fractionated phytigel solutions. The organic substances in these samples were characterized by measuring the concentrations of reduced sulfur species (RSS), amino/thio groups (CPSA), surface active substances (SAS), TEP and different components of carbohydrates. All metal additions and respective measurements were conducted in triplicate, except when noted otherwise.

Preparations of samples

Marine diatom cultures. Cultures of the two marine diatoms, *Skeletonema costatum* and *Thalassiosira weissflogii* and the coccolithophorid *Emiliania huxleyi* were grown in f/2 media at 15 °C, under a 16: 8 light: dark cycle at 30 to 40 $\mu\text{mol m}^{-2} \text{s}^{-1}$ light . The f/2 media (Guillard and Ryther, 1962) was based on filtered (0.45 μm nitrocellulose membrane, Millipore) seawater from the North Sea. The whole cultures were collected and used in their stationary phase at cell concentrations of app. 5×10^6 cells/L. At this time cells had released large amounts of organic substances into the water, many of which may act as ligands for copper or cadmium. The cultures were used either undiluted and/or after dilution with a NaCl – Milli-Q solution (0.55M) at a dilution factor of 1: 5 by volume (10 mL culture in 50 mL total volume).

Solutions of phytigel. Phytigel, which is an agar substitute produced from a bacterial substrate composed of glucuronic acid, rhamnose and glucose, was used as a model polysaccharide compound. Phytigel (Sigma), has an average molecular weight of 1000 kDa and produces a clear colorless gel in seawater. A stock solution of 1g/L of phytigel was prepared in Milli-Q water and was homogenized in an ultrasonic bath. An unfiltered solution

as well as two filtrates (0.2 and 0.7 μm , respectively, Millipore) of phytagel were analyzed electrochemically. For SWV scans and CLE-CSV laminarin, carrageenan and alginic acid were dissolved in artificial seawater containing 0.55M NaCl and adjusted to pH 8.

Analysis

Complexing capacity determinations with Cu and Cd. Differential pulse anodic stripping voltammetry (DPASV) is considered particularly suitable for measuring Cu and Cd concentrations in seawater (Plavšić et al., 1982; Ellwood, 2004, Scoullos et al., 2006) and was used for the determination of the respective complexing capacities, CCu and CCd, as well as the corresponding apparent stability constants (K_{app}) (Ružić, 1982; van den Berg, 1982).

The complexing capacity values were determined by direct titration of 25 ml of sample with copper or cadmium ions. Figure 3 illustrates the determination of the complexing capacity using the example of *S. costatum*. Figure 3a presents results of the anodic stripping voltammetric waves for copper ion titration, where increasing amounts of copper ions (8 – 260 nmol L⁻¹ Cu) were added to a diluted culture (1: 5) of *S. costatum*. Upon additions of copper, the Cu peak increased. In Figure 3b the concentrations of the added copper ions is depicted on the x axis vs. the retrieved (measured) copper ion concentrations for each addition of Cu ion to pure electrolyte (0.55M NaCl) (open circles) or to the *S. costatum* culture (full circles). The difference between the two lines when extrapolated to the x-axis gives the approximate value of the copper complexing capacity (CCu). The exact value of the CCu can be calculated from the regression of the Cu ion measured (on x-axis) vs. the Cu ion measured normalized to the complexed Cu as shown in Figure 3c. The concentration of complexed Cu was calculated from $\text{Cu}_{\text{total}} - \text{Cu}_{\text{measured}}$. The inverse of the slope gives the CCu while K_{app} (apparent stability constant) is obtained from the intercept on the y-axis (Ružić, 1982; van den Berg, 1982). Every addition of metal ion to the sample solution was

measured three consecutive times. The complexing capacities of the diluted and undiluted cultures were identical, indicating that this parameter is independent of dilution.

Identification of Fe complexes of laminarin, carrageenan and alginic acid using SWV. Scans were performed in the region of -0.2 to -1.8 V methods' upper limit determined by the oxidation of Hg and lower limit by the formation of H₂ using a hanging mercury drop electrode without a deposition step, since uncomplexed Fe can not be accumulated electrochemically on the mercury. Omitting a deposition step requires working with high Fe concentrations (10^{-6} M) as the sensitivity is low.

Determination of apparent stability constants of Fe complexes of laminarin, carrageenan and alginic acid using CLE-CSV. The Fe binding strength of the dissolved PS was investigated using CLE-CSV as described by Croot et al. (2000). In short, each PS containing solution was titrated with Fe and the portion of Fe not complexed by the PS but bound to the competing ligand 2-(2-Thiazolylazo)-p-cresol (TAC) was measured. TAC is an Fe ligand of known strength added to the sample in a known concentration. Fe reaches an equilibrium distribution between the PS and TAC according to the concentration of each constituent and the stability constant of each complex. The Fe-TAC complex can be measured electrochemically, as it induces a current when reduced on the electrode, whereas the potential Fe-PS complex cannot. This method has a detection window of conditional stability constants (k') of competing Fe ligands which ranges from $\log k'_{FeL} = 21.4$ to 23.4 ($10 \mu\text{M}$ TAC), depending on the concentration of added TAC.

The titration curve (i.e. added Fe vs. reduction current) can be evaluated by fitting a model of the competitive equilibrium in the solution, hence retrieving the values of the unknown parameters, i.e. the stability constant of the Fe-PS complex and the concentration of PS. The

general pattern of a titration curve consist of an initial non-linear phase until the competing ligand (e.g. PS) is saturated with Fe, followed by a linear phase titrating only TAC, which is added to the sample in excess over the concentration of competing ligand and added Fe.

Determination of reduced sulfur species (RSS). RSS were determined by square wave cathodic stripping voltammetry (SWV; Ciglenečki and Čosović 1996). Measurements were performed with a µ-Autolab analyzer (Electrochemical Instruments, Eco Chemie) connected to a 663 VA stand (Metrohm), with an SMDE (static mercury drop electrode) as the working electrode. The reference electrode was an Ag/AgCl (3 M KCl) electrode connected to the solution via an electrolyte bridge. A platinum electrode served as the auxiliary electrode. Electrochemical determination of RSS is based on the reaction between sulfur and the mercury electrode. Measurements were conducted before and after purging the 50ml solution of phytagel or culture with N₂ gas to determine if some fraction of the RSS was present as sulfides. The samples were measured immediately after preparation and as purgable S species were removed after the first scan, replicate measurements of the initial pre-purge values were not performed. After accumulation of RSS on the electrode surface at a deposition potential of E = -0.20 V (vs. Ag/ AgCl) from a stirred solution, we ran potential scans in the negative direction (up to E = -1.00 V vs Ag/AgCl). HgS reduction peaks that are characteristic for many RSS were recorded (Ciglenečki and Čosović, 1996). Then the solution was acidified (pH=2.0), purged with N₂ and after that the pH was readjusted back to pH=8.0 and, the RSS signal recorded again. Samples were not readjusted to exactly the original pH. Re-adjustment was done in the electrochemical cell, so approximate concentrations either of HCl or NaOH were added according to the previous experiment. As a consequence the signal of RSS as seen in the voltammogram differed slightly between the original and pH adjusted sample.

Sulfur species concentration is expressed as equivalents of glutathione, determined from the calibration with glutathione. Glutathione was chosen for calibration because of its electrochemical similarity with the sulfur species observed in the three cultures, i.e. the half-wave potential of appearance and behavior upon pH changes were similar (Ciglenečki and Ćosović, 1996).

Constant-current chronopotentiometric stripping analysis (CPSA) for the determination of amino/thio groups. Constant-current CPSA produces well-resolved current peaks, ‘presodium’ currents with the static mercury drop electrode (SMDE) that are characteristic for proteins and other compounds with –SH and –NH₂ groups (Tomschik et al.1999; Mader et al.2001). Accumulation of the catalytically active compound at the SMDE polarized to a potential E = -0.20 V, was achieved by stirring the solution for 60 s (accumulation time, t_a).After a quiescent period of 10 s, a constant stripping current of I = -1 μA intensity was passed through the electrolytic circuit, and constant-current CPSA curves were recorded. These measurements were carried out in samples previously purged with N₂

Surface-active substances (SAS). SAS were determined with phase-sensitive alternating current voltammetry (Ćosović and Vojvodić, 1987). This electrochemical method measures the capacitive current (i.e. the current arising from adsorption processes, measured out-of-phase with the applied potential) separately from the faradaic current (originating from redox processes, measured in-phase with the applied potential). Out-of-phase measurements have found wide application in the study of organic substances with surface-active properties in marine and freshwater systems. The decrease in the capacitive current in the presence of surface-active organic material below the value for the pure electrolyte solution indicates the amount of this material adsorbed onto the electrode (and can be expressed quantitatively by

an equivalent amount of a selected SAS, e.g. Triton-X-100). The shape of the voltammetric curves recorded (i.e. current vs. potential) is characteristic for the substance investigated.

Samples were calibrated against the nonionic SAS, Triton-X-100. Prior to measurements, samples were thoroughly homogenized by stirring.

TEP determinations. TEP (transparent exopolymer particles) were analyzed colorimetrically (Passow and Alldredge, 1995). Six replicate samples of 50 ml each were filtered onto 0.4 µm polycarbonate filters (Poretics) and stained with Alcian blue. Gum Xanthan was used as a calibration standard and results are expressed as Gum Xanthan equivalent per Liter (GX eq. L⁻¹).

Carbohydrate determinations. Carbohydrates (polysaccharides plus monosaccharides) were determined for the whole sample (dissolved + particulate fraction) and for the dissolved fraction (< 0.4 µm) according to Myklestad (Myklestad et al., 1997). Between 10 and 20 ml sample were filtered through a 0.4 µm filter for the determinations of dissolved carbohydrates. Total (dissolved + particulate) and dissolved MS (monosaccharides), respectively were determined in 1 ml each (triplicates) of unfiltered and in 1ml each (triplicates) of 0.4 µm filtered sample. Four ml of filtered and unfiltered sample were hydrolyzed and the total carbohydrate content was measured. The PS (polysaccharide) concentration was determined by subtracting the MS concentration from the total carbohydrate concentration. This method, which measures both, neutral and charged carbohydrates, subjects the saccharides to an oxidation reaction at alkaline pH, during which Fe³⁺ is reduced to Fe²⁺. The Fe²⁺ is then determined colorimetrically after condensation with the cromogen 2,4,6-trypyridyl-s-triazine (TPTZ) and formation of the purple color of Fe(TPTZ)₂²⁺.

RESULTS AND DISCUSSION

Complexing capacity and stability constant for Cu and Cd complexation

In Table 1 the results of the complexing capacity measurements for Cu and Cd for the three phytoplankton cultures and the model substance phytagel are presented. The complexing capacity for copper ions was highest in the *T.weissflogii* (1.14 µM) and the *S. costatum* cultures (1.06 µM) while it was an order of magnitude lower (0.14 µM) in the culture of *E.huxleyi*. In the culture of *E.huxleyi* the complexing capacity for cadmium ions was, however, twice that of those of *T.weissflogii* and the *S. costatum* (0.04 vs. 0.02 µM and 0.02 µM, respectively). Appreciably lower CCd values compared to CCu values are common (Scoullos et al , 2004, Scoullos et al., 2006). Complexing capacities for both Cu and Cd were lower in the 5 mg L⁻¹ phytagel solution than in those stemming from phytoplankton cultures. In both diatom cultures, the apparent stability constant for Cd was higher than that for Cu, indicating more specific binding places for Cd ions compared to Cu ions. More specific binding for Cd is also supported by the lower complexing capacity for Cd, as more specific sites are rarer (Gordon et al., 2000; Laglera and Berg, 2003).

A CCu of 0.33 µM was obtained for the unfiltered phytagel solution, whereas the CCu after filtration through either 0.2 µm or 0.7 µm was 73% lower at 0.09 µM, suggesting that particles larger 0.7 contributed most significantly to binding Cu. Natural marine Cu-complexing ligands have been found to belong to 50% to substances between 1 and 10 kDa (Wells et al., 1998b; Wen et al., 1999), implying colloidal aggregation or gelation of Cu complexing ligands or adsorption of Cu to gel-particles in our phytagel solution. Our analysis method can't differentiate between complexation and adsorption onto particles. Alternatively

the complexing substances absorbed to the filter thus retaining them although their molecular weight should have allowed them to pass.

Cd has been detected mainly complexed to organic matter in the low molecular weight fraction < 1k Da (Grzybowski, 2000; Wells et al., 1998a). In our phytagel solution filtration (by either 0.2 μm or 0.7 μm) reduced the CCd by only 33%, indicating that in our phytagel solution Cd complexed mostly with substances passing a 0.2 μm filter. Clearly ligands complexing Cu and Cd differed even in our model phytagel solution.

Identification of Fe complexes of laminarin, carrageenan and alginic acid using SWV

Initial scans performed in artificial seawater containing only 0.5 mM BisTris buffer (pH 8) revealed a peak at -1.4 V which increased linearly (Fig. 1a) when adding Fe (0-15 μM). The sensitivity was 1.4 nA μM^{-1} . Apart from buffering the pH, BisTris buffer also slightly complexes Fe and prevents hydrolysis and precipitation of Fe (Taylor, Chelate scale paper). Hydrolysis and formation of less soluble Fe hydroxides shows a quadratic or cubic relationship to the Fe concentration and is even more sensitive to increasing pH. This explains further scans of artSW, without BisTris buffer present, which did not show any Fe peak at pH 6-8. However, lowering the pH to 4 resulted in a peak at -1.6 to -1.7 V, which changed with changing Fe concentrations, but not systematically.

SWV scans (Fig. 1b) of laminarin (2 g L^{-1}) and alginic acid (2 g L^{-1}) dissolved in artificial seawater at pH 8 also showed no peak from -0.2 to -1.8 V, i.e. there was no dissolved Fe species present that could be reduced. At pH 4-8 carrageenan (0.1 g L^{-1}) caused spike like peaks at -0.5 and -0.75 V (Fig. 1b) which can be related to the sulphur contained in the side chains of this mucopolysaccharide (M. Plavsic, pers. comm). No peaks at -1.4 to -1.7 V could be detected.

Determination of apparent stability constants of Fe complexes of laminarin, carrageenan and alginic acid using CLE-CSV.

The titration data of all analysed PS over a range of 0.02 to 0.5 mg L⁻¹ did not show a curvature (Fig. 2) consequently, no stability constant could be determined. Even reducing the TAC concentration by 50%, to lower the detection window and shift the equilibrium more towards the Fe-PS complex, showed very similar result. The titration data showed generally a lower slope (Fig. 2) than the reference sample, which was UV treated organic-free seawater (UVSW).

The titrations of PS solutions of up to 0.5 mg L⁻¹ did not yield any k' values, indicating that these PS bind Fe only weakly ($\log k' < 21.4$) if at all. Confirming the above results that did not show any specific Fe comlexation either. However, the inability to determine these k' values may have been due to the fact that sensitivity of the method was hindered by the PS themselves.

Characterization of organic matter in culture media

Concentrations of sulfur species: All three cultures contained different concentrations of sulfur (Table 1), with by far highest concentrations in the media stemming from *T. weissflogii*. Some fraction of the RSS in this culture must have been present as sulfides, as indicated by the fact that some part of the sulfur species was purged with N₂ gas. The original SWV voltammogram for *T. weissflogii* exudates was almost halved upon acidification, purging with N₂ and readjustment of the pH back to pH = 8.1 (Fig. 4a). This decrease in sulfur was due to the presence of sulfur species that were purged with N₂ gas. The peak potential after the readjusting of the pH is a little bit shifted towards more negative potential (from -0.6 to -0.65), because the reaction is very sensitive to small changes in pH (Ciglenečki and Čosović, 1996). The original square wave voltammogram for the *S. costatum* culture (Fig. 4b)

remained the same upon acidification to pH =2, purging with N₂, and readjustment of pH back to 8.1 indicating the presence of sulfur species that could not be purged by N₂ gas only. The culture of *E. huxleyi* (not shown) behaved the same as the *S. costatum* culture, i.e. the sulfur voltammetric peak did not change upon acidification and purging, indicating the absence of purgable sulfur species. Assuming that about half of the sulfur in the *T. weissflogii* culture was purgable the concentration of organic, non purgable sulfur was still highest in the culture of *T. weissflogii* compared to *S. costatum* and *E. huxleyi*. These non-purgable sulfur species of all three cultures electrochemically resembled glutathione, suggesting this substance class to be abundant in all three cultures. Glutathione and other thiols are present in surface waters, and are known to be released by phytoplankton, including *E. huxleyi* (Dupont and Ahner, 2005) and *T. weissflogii* (Tang et al., 2005) when exposed to elevated concentrations of Cu or Cd.

Presence of NH₂ and/or sulfur groups: The CPSA method determines the presence of NH₂ or sulfur containing groups, that may be present in different macromolecular compounds e.g. in amino acids, proteins, polysaccharides (Tomschik et al., 1999, Mader et al. 2001, Ciglenečki et.al., 2003). Of our cultures and the phytagel, only the *S. costatum* culture showed the characteristic “presodium” wave (Fig. 5) indicating the catalytic effect of –NH₂ and/or sulfur groups. Voltammetric peaks 5 and 6 (Fig. 5) were obtained by prolonged accumulation (180 s and 300 s) of *S. costatum* and are situated at the potential of ~ -1.7 V. For shorter accumulation times the peaks were not so pronounced. The appearance of the voltammetric current peak at ~ -1.7V vs. ref. Ag/AgCl electrode indicates the presence of –NH₂ groups, while for PS with sulphur groups, such as carrageenans, a more positive catalytic voltammetric peak would have been observed (at -1.4 V to -1.5 V) (Plavšić and Ćosović, 1998, Ciglenečki et al., 2003). It is known that in *S. costatum* culture during the onset

and development of the bloom 60-80 % of total complexing agents exuded could be ascribed to “protein-like” compounds which could explain the observed voltammetric peak at – 1.7 V (Lorenzo et al., 2007).

Surface active substances: The characteristic AC (alternating current) out of phase voltammetric curves for the three phytoplankton cultures and the model compounds phytigel, laminarin, carrageenan and alginic acid showed the suppression of the capacity current in comparison to the capacity current of the pure electrolyte (0.55 M NaCl) (Fig. 6). This difference in the shape of the curves of the electrolyte compared to the phytoplankton cultures indicate the presence of natural, heterodispersed polysaccharids in the cultures (i.e. at negative potentials (~-1.6 to -1.8 V) the a.c. voltammetric curves of a cultures are not smooth like for the electrolyte solution)(Plavšić et al, 1990). The a.c. scans of solutions of phytigel, laminarin, carrageenan and alginic acid showed a pronounced desorption wave at a potential range from ~-0.7 V to -1.4 V, which is characteristic of synthetic surfactants, like Triton-X-100 or sodium dodecyl sulfate, although some SAS of natural origin like fatty acids may also exhibit pronounced desorption waves (Ćosović, 1985).

The highest concentration of SAS in the phytoplankton samples was observed in the culture of *E. huxleyi* (0.26 mg/L eq. Triton-X-100) followed by *S. costatum* (0.24 mg/L eq Triton-X-100) and *T. weissflogii* (0.18 mg/L eq. Triton-X-100) (Table 1, Fig. 6A). The same amount of SAS was also measured in *E. huxleyi* in stationary phase by Ciglenečki and Ćosović (1996). The comparison of phytigel, laminarin, carrageenan and alginic acid (Fig. 6B) showed highest surface activity for laminarin, decreasing via phytigel, alginic acid and carrageenan.

TEP and carbohydrates: The total (dissolved + particulate) carbohydrate (polysaccharide + monosaccharide) concentration ranged between 1.2 and 3.6 mg glucose equivalent L⁻¹, of which 53%, 57%, 79% and 98% belonged to the dissolved (<0.4 µm) pool in phytigel, *T. weissflogii*, *E. huxleyi* and the *S. costatum*, respectively (Fig. 7). Less than 40% of the carbohydrates were polysaccharides in *E. huxleyi* and *S. costatum*, whereas polysaccharides dominated the carbohydrate pool in *T. weissflogii* (> 60%) or the phytigel solution (> 80%). Polysaccharide concentrations ranged between 0.5 and 2.5 mg glucose eq. L⁻¹ in the cultures and phytigel solution, with higher values in the unfiltered compared to the 0.4 prefiltered samples (Fig. 7). Concentrations of dissolved polysaccharides were highest in *T. weissflogii* (1.3 mg glucose eq. L⁻¹), followed by *E. huxleyi* (0.8 mg glucose eq. L⁻¹) and *S. costatum* (0.7 mg glucose eq. L⁻¹) and lowest in phytigel (0.3 mg glucose eq. L⁻¹). Particulate polysaccharides were highest in *T. weissflogii* and phytigel and almost absent in *S. costatum* (Fig. 7).

TEP concentrations were highest in the phytigel solution (6500 mg xanthan eq/L), followed by the media of *E. huxleyi* (2300 mg xanthan eq/L) and *T. weissflogii* (1000 mg xanthan eq/L) with the lowest concentration in culture media of *S. costatum* (400 mg xanthan eq/L) and reflected neither the pattern of particulate polysaccharide, nor that of SAS (Fig. 7).

Characteristics of DOM and its relationship to Cu- and Cd-complexing capacity

We characterized the organic material, which could be responsible for the binding of Cu or Cd, by measuring sulfur content, SAS, poly- and monosaccharides (in their particulate and dissolved phase) and TEP. Each of these measurements characterizes a certain fraction of DOM, but none of these fractions are well characterized and the degree of overlap between these pools is unknown.

Our data suggest that in our cultures and phytagel, TEP concentration was not correlated with either the carbohydrate fractions, nor with SAS or sulfur concentrations. The lack of a correlation with polysaccharides confirms that acidic polysaccharides are a varying fraction of total polysaccharides. The lack of a correlation between TEP and SAS suggests that not all TEP are surface active and that other substances besides TEP are responsible for the binding of trace elements. TEP are rich in sulfur (Zhou et al., 1998), but our samples clearly contained other substances rich in sulfur as TEP and sulfur concentrations showed no correlation. The correlation between PS and sulfur ($PS < 0.4 \mu\text{m}$: $r = 0.94$, $p < 0.01$, $n = 3$, $PS > 0.4\mu\text{m}$: $r = 0.91$, $p < 0.05$, $n = 3$) suggests that a significant fraction of this total amount of sulfur was associated with non acidic polysaccharides. Electrochemical characterizations suggested glutathione type substances to be responsible for the high sulfur content.

SAS were negatively correlated both with dissolved PS ($r = 0.96$, $p < 0.001$, $n = 4$) and sulfur content ($r = 0.99$, $p < 0.0005$, $n = 3$), implying that SAS in our samples consisted of sulfur-poor substances other than polysaccharides. SAS generated by phytoplankton can be rich in proteinaceous substances (Gašparović et al., 2007).

Although our RSS measurements suggest the presence of glutathione type substances in all three cultures, exudates of all three cultures differed in their other characteristics. A comparison between them shows that *T. weissflogii* cultures contained large amounts of both, purgeable and non-purgeable sulfur, high concentrations of polysaccharides (both dissolved and particulate), but relatively low TEP concentrations. *S. costatum* where CCu was similarly high, was characterized by fairly high concentrations of non-purgable sulfur, and low concentrations of particulate carbohydrates (both polysaccharides and monosaccharides) and TEP. The presence of NH₂ groups further characterized *S. costatum* exudates. Assuming the main CCu ligand in both diatom cultures was the same, it was not measured as TEP and did not contain NH₂ groups, but could have been included in determinations of RSS, SAS and

dissolved polysaccharides. Organic matter of *E. huxleyi*, which had a relatively high CCd was characterized by high concentrations of monosaccharides (both particulate and dissolved) and relatively low sulfur content.

Assuming the main respective Cu or Cd binding ligand in the three cultures and in the phytagel solution belonged to the same substance group and contributed significantly to that group, a relationship between the complexing capacity and the concentration of that substance group is expected. In our experiments however, TEP concentration was not correlated to the binding capacity or the stability constants for Cu or Cd. SAS, another candidate as a trace metal ligand were also not correlated to either Ccu or Ccd. So both TEP and SAS appeared not to have been responsible for the observed complexing capacities of Cu or Cd.

Carbohydrates (poly- or monosaccharides) could also not explain the observed binding capacities of Cu or Cd, except that the monosaccharide concentration was positively correlated to CCd ($MS < 0.4 \mu\text{m}$: $r = 0.95$, $p < 0.005$, $n = 4$, $MS > 0.4 \mu\text{m}$: $r = 0.85$, $p < 0.05$, $n = 4$). Thus our data suggests that MS were primarily responsible for the complexing capacity of Cd in all samples. A glutathione-type ligand was found in all three cultures. Assuming that about half of the sulfur in the culture of *T. weissflogii* belonged to this ligand (half was purgeable) a significant (RSS *T. weissflogii*: 90 GSSG eq. nM, $r = 0.94$, $p < 0.01$, $n = 3$) positive relationship between RSS and CCu is found, indicating that this glutathione type ligand could have been responsible for the binding of Cu in all three cultures.

The apparent absence of significant amounts of ligands in TEP or SAS could have several reasons. Either, no ligand of importance belonged to these groups of substances. Or, alternatively a potential ligand belonging to TEP or SAS made up only a small fraction of TEP or SAS, which was lost in the noise of the bulk measurement. Both TEP and SAS are operationally defined groups of organic substances, containing a large variety of chemically

different molecules. Unfortunately this implies that we need to find better methods to characterized metal binding ligands more specifically.

CONCLUSION

The three phytoplankton cultures and the phytagel solution used as a model, complexed copper ions and to a lesser extent also cadmium ions. The apparent stability constants were higher for cadmium ions than for Cu showing that Cd binding places are more specific. No apparent stability constant for iron could be determined for laminarin, carrageenan and alginic acid. Nevertheless these polysaccharides showed high surface activity which agrees with reported abiotical formation of TEP from acidic polysaccharides (Passow). Some ligands in the phytoplankton cultures belonged to the “glutathione” type. These might have been responsible for the binding of Cu. Monosaccharide concentrations correlated with CCd, implying that the Cd ligand belonged to this group of molecules. None of the other measured substance classes assumed to be potentially important ligands (TEP, SAS, polysaccharides) could be identified as being primarily responsible for the complexing properties in all cultures, suggesting a high variability in space and time with regards to the chemical substances responsible for the binding. The absence of correlations between the complexing capacity and TEP, SAS, carbohydrates in our measurements contradict the belief that these substance groups contain the majority of trace metal binding ligands.

LITERATURE

- Aluwihare L.I, Repeta D.J., 1999. A comparison of the chemical characteristics of oceanic DOM and extracellular DOM produced by marine algae. *Mar. Ecol. Prog. Ser.* 186, 105-117.
- Aluwihare, L., Repeta, D., Chen, R., 1997. A major biopolymeric component of dissolved organic carbon in surface sea water. *Nature* 387, 166-169.
- Benner, R., 2002. Chemical composition and reactivity. In: Hansell D.A., Carlson, C. (Eds.), *Biogeochemistry of dissolved organic matter*. Academic Press, Elsevier Science, New York, 59-90.
- Benner, R., Pakulski, J.D., McCarthy, M., Hedges, J., Hatcher, P., 1992. Bulk chemical characteristics of dissolved organic matter in the ocean. *Science* 255, 1561-1564.
- Blake, A.C., Chadwick, D.B., Zirino, A., Rivera-Duarte, I., 2004. Spatial and temporal variations in copper speciation in San Diego Bay. *Estuaries* 27 (3), 437-447.
- Bruland, K.W., Donat, J.R., Hutchins, D.A., 1991. Interactive influence of bioactive tracemetsals on biological production in oceanic waters. *Limnol. Oceanogr.* 36, 1555-1577.
- Bruland, K.W., 1992. Complexation of cadmium by natural organic ligands in the central North Pacific. *Limnol. Oceanog.* 37 (5), 1008-1017.
- Buck, K. and Bruland, K., 2005. Copper speciation in San Francisco Bay: A novel approach using multiple analytical windows. *Mar. Chem.* 96, 185-198.
- Buckley, P., van den Berg, C.M.G., 1986. Copper complexation profiles in Atlantic Ocean. *Mar. Chem.* 19, 281-296.
- Ciglenečki, I., Čosović, B., 1996. Electrochemical study of sulfur species in seawater and marine phytoplankton cultures. *Mar. Chem.* 52 (1), 87-97.
- Ciglenečki, I., Čosović, B., Vojvodić, V., Plavšić, M., Furić, K., Minacci, A., Baldi, F., 2000. The role of reduced sulfur species in the coalescence of polysaccharides in the Adriatic Sea. *Mar. Chem.* 71, 233-249.
- Ciglenečki, I., Plavšić, M., Vojvodić, V., Čosović, B., Pepi, M., Baldi, F., 2003. Evidence of mucopolysaccharide transformation by sulfide: comparisons between an enriched mixed benthic diatom culture and natural mucilage. *Mar. Ecol. Prog. Ser.* 263, 17-27.
- Čosović, B., 1985. Aqueous surface chemistry. Adsorption characteristics of organic solutes. *Electrochemical evaluation*, in: W. Stumm (Eds.), *Chemical Processes in Lakes*. J. Wiley and Sons, New York, pp. 55-85.

- Ćosović, B., 2005. Surface Active properties of the sea surface microlayer and consequences for pollution in the Mediterranean Sea, in: Saliot, A. (Eds.), The Mediterranean Sea, The Handbook of Environmental Chemistry. Springer, pp. 269- 297.
- Ćosović, B., Vojvodić, V., 1987. Direct determination of surface active substances in natural waters. Mar. Chem. 22, 363-373.
- Dryden, C.L., Gordon, A.S., Donat, J.R., 2007. Seasonal survey of copper-complexing ligands and thiol compounds in a heavily utilized, urban estuary: Elizabeth River, Virginia. Mar. Chem. 103 (3-4), 276-288.
- Dupont, C.L., Ahner, B.A., 2005. Effects of copper, cadmium and zinc on the production and exudation of thiols by *Emiliania huxleyi*. Limnol. Oceanogr. 50 (2), 508-515.
- Elwood, M., 2004. Zinc and cadmium speciation in subantarctic waters east of New Zealand. Mar. Chem. 87, 37-58.
- Gašparović, B., Plavšić, M., Bošković, N., Ćosović, B., Reigstad, M., 2007. Organic matter characterization in Barents Sea and eastern Arctic Ocean during summer. Mar. Chem. 105 (1-2), 151-165.
- Gimenez, M., Arino, C., Esteban, M., 1995. Voltammetry of Pb(II), Cd(II) and Zn(II) ions in the presence of sulfated polysaccharide λ - carrageenan. Anal. Chim. Acta. 310, 121-129.
- Gordon, S.A., Donat, J.R., Kango, R.A., Dyer, B.J., Stuart. M.L., 2000. Dissolved copper-complexing ligands in cultures of marine bacteria and estuarine water. Mar. Chem. 70, 149-160.
- Grzybowski, W., 2000. Comparison between stability constants of cadmium and lead complexes with humic substances of different molecular weight isolated from Baltic Sea water. Oceanologia 42 (4), 473-482.
- Guo, L., Hung, C.C., Santschi, P.H., Walsh, I.D., 2002. ^{234}Th scavenging and its relationship to acid polysaccharide abundance in the Gulf of Mexico. Mar. Chem. 78, 103-119.
- Honeyman, B., Santschi, P., 1991. Coupling adsorption and particle aggregation: laboratory studies of "colloidal pumping" using ^{59}Fe -labeled hematite. Environmental science and technology 25 (10), 1739-1747.
- Kim, Y., Yoo, Y., Lee, H., 1995. Characteristics of lead adsorption by *Undaria pinnatifida*. Biotechnological letters 17, 345-350.

- Kozarac, Z., Plavšić, M., Čosović, B., Viličić, D., 1989. Interaction of cadmium and copper with surface active organic matter and complexing ligands released by marine phytoplankton. Mar. Chem. 26, 313-330.
- Laglera, L.M., van den Berg, C.M.G., 2003. Copper complexation by thiol compounds in estuarine waters. Mar. Chem. 82, 71-89.
- Laglera, L.M., van den Berg, C.M.G., 2006. Photochemical oxidation of thiols and copper complexing ligands in estuarine waters. Mar. Chem. 101 (1-2), 130-140.
- Leal, M.F.C., Vasconcelos, M.T.S.D., van den Berg, C.M.G., 1999. Copper – induced release of complexing ligands similar to thiols by *Emiliania huxleyi* in seawater cultures. Limnol. Oceanogr. 47 (7), 1750-1762.
- Liss, P.S., Duce, R.A., 1997. The Sea Surface and Global Change, Cambridge University Press, Cambridge, United Kingdom.
- Lorenzo, J.I., Nieto-Cid, M., Alvarez-Salgado, X.A., Perez, P., Beiras, R. 2007. Contrasting complexing capacity of dissolved organic matter produced during the onset, development and decay of a simulated bloom of the marine diatom *Skeletonema costatum*. Mar. Chem. 103, 61-75.
- Mader, P., Vesela, V., Dorčak, V., Heyrovský, M., 2001. The ‘presodium’ hydrogen evolution at the dropping mercury electrode catalyzed by simple cysteine peptides. Collect. Czech Chem. Commun. 66, 397–410.
- Mopper, K., Zhou, J., Ramana, K. S., Passow, U., Dam, H.G., Drapeau, D.T., 1995. The role of surface-active carbohydrates in the flocculation of a diatom bloom in a mesocosm. Deep-Sea Research II. 42, 47-73.
- Muller, F.L.L., Jacquet, S.P., Wilson, W.H., 2003. Biological factors regulating the chemical speciation of Cu, Zn, and Mn under different nutrient regimes in a marine mesocosm experiment. Limnol. Oceanogr. 48 (6), 2289-2302.
- Myklestad, S.M., Skanoy, E., Hestmann, S., 1997. A sensitive and rapid method for analysis of dissolved mono- and polysaccharides in seawater. Mar. Chem. 56 (3-4), 279-286.
- Passow, U., Alldredge, A.L., 1994. Distribution, size, and bacterial colonization of transparent exopolymer particles (TEP) in the ocean. Mar. Ecol. Prog. Ser. 113, 185-198.
- Passow, U., Alldredge, A.L., 1995. A dye-binding assay for the spectrophotometric measurement of transparent exopolymer particles (TEP). Limnol. Oceanogr. 40, 1326-1335.

- Passow, U., 2000. Formation of Transparent Exopolymer Particles, TEP, from dissolved precursor material. *Mar. Ecol. Prog. Ser.* 192, 1-11.
- Passow, U., 2002. Transparent exopolymer particles (TEP) in aquatic environments. *Progress in Oceanography* 55, 287-333.
- Passow, U., 2004. Switching perspectives: Do mineral fluxes determine particulate organic carbon fluxes or vice versa. *Geochemistry, Geophysics, Geosystems* 5, 1-5.
- Passow, U., Dunne, J., Murray, J.W., Balistrieri, L.S., Alldredge, A.L., 2006. Organic carbon to ^{234}Th ratios of marine organic matter. *Mar. Chem.* 100, 323-336.
- Plavšić, M., Krznarić, D., Branica, M., 1982. Determination of the apparent copper complexing capacity of seawater by anodic stripping voltammetry. *Mar. Chem.* 11, 17-31.
- Plavšić, M., Vojvodić, V., Čosović, B., 1990. Characterization of surface active substances during a semi-field experiment of a phytoplankton bloom. *Anal. Chim. Acta* 232, 131-140.
- Plavšić, M., Čosović, B., 1998. Adsorptions of carrageenans on mercury surface in sodium chloride solution and seawater. *Croat. Chem. Acta* 72 (2), 233-243.
- Plavšić, M., 2003. Electroanalytical techniques applied for studying the interaction of organic matter and particles with metal ions in natural waters. *Analytical Letters* 36 (1), 43-157.
- Plavšić, M., Lee, C., Čosović, B., 2006. Copper complexing properties of melanoidins and marine humic material. *Science of the Total Environment* 366, 310-319.
- Quigley, M.S., Santschi, P.H., Guo, L., Honeyman, B.D., 2001. Sorption irreversibility and coagulation behavior of ^{234}Th with marine organic matter. *Mar. Chem.* 76, 27-45.
- Quigley, M.S., Santschi, P.H., Hung, C.C., Guo, L., Honeyman, B.D., 2002. Importance of acid polysaccharides for ^{234}Th complexation to marine organic matter. *Limnol. Oceanogr.* 47, 367-377.
- Ross, A.R.S., Ikonomou, M.G., Orians, K.J., 2003. Characterization of copper complexing ligands in seawater using immobilized copper (II)-ion affinity chromatography and electrospray ionization mass spectrometry. *Mar. Chem.* 83, 47-58.
- Ružić, I., 1982. Theoretical aspects of the direct titration of natural waters and its information yield for trace metal speciation. *Anal. Chim. Acta* 140, 99-113.
- Santschi, P.H., Murray, J.W., Baskaran, M., Benitez-Nelson, C.R., Guo, L.D., Hung, C.C., Lamborg, C., Moran, S.B., Buesseler, K.O., Passow, U., Roy-Barman, M., 2006. Thorium speciation in seawater. *Mar. Chem.* 100, 250-268.

- Scoullos, M., Plavšić, M., Karavoltsos, S., 2004. Copper speciation in the Gulf of Elefsis, The role of macroalgae *Ulva rigida*. Mar. Chem. 86, 51-63.
- Scoullos, M., Plavšić, M., Karavoltsos, S., Sakellari, A., 2006. Partitioning and distribution of dissolved copper, cadmium and organic matter in Mediterranean marine coastal areas: The case of a mucilage event. Estuarine, Coastal and Shelf Science 67, 484-490.
- Tang, D., Shafer, M.M., Karner, D.A., Armstrong, D.E., 2005. Response of nonprotein thiols to copper stress and extracellular release of glutathione in the diatom *Thalassiosira weissflogii*. Limnol. Oceanogr. 50 (2), 516-525.
- Tomschik, M., Jelen, F., Havran, L., Trnkova, L., Nielsen, P.E., Paleček, E., 1999. Reduction and oxidation of peptide nucleic acid and DNA at mercury and carbon electrodes. J. Electroanal. Chem. 476, 71–80.
- Van den Berg, C.M.G., 1982. Determination of copper complexation with natural organic-ligands in sea-water by equilibration with MnO₂: I. Theory. Mar. Chem. 11, 307-322.
- Verdugo, P., Alldredge, A.L., Azam, F., Kirchman, D., Passow, U., Santschi, P., 2004. The oceanic gel phase: a bridge in the DOM-POM continuum. Mar. Chem. 92, 67-85.
- Wells, M.L., Goldberg, E.D., 1994. The distribution of colloids in the North Atlantic and Southern Oceans. Limnol. Oceanogr. 39, 286-302.
- Wells, M.L., Kozelka, P.B., Bruland, K.W., 1998. The complexation of 'dissolved' Cu, Zn, Cd and Pb by soluble and colloidal organic matter in Narragansett Bay, RI. Mar. Chem. 62 (3-4), 203-217.
- Wen, L.-S., Santschi, P., Gill, G., Paternostro, C., 1999. Estuarine trace metal distributions in Galveston Bay: Importance of colloidal forms in the speciation of the dissolved phase. Mar. Chem. 63 (3-4), 185-212.
- Zhou, J., Mopper, K., Passow, U., 1998. The role of surface-active carbohydrates in the formation of transparent exopolymer particles by bubble adsorption of seawater. Limnol. Oceanogr. 43, 1860-1871.

Acknowledgement:

The authors thank the Deutsche Forschung Gemeinschaft (DFG, KRO 436) for funding that made the collaboration between the AWI and the IRB possible. M.P and S.S. are also supported by the Croatian Ministry of Science, Education and Sport (Project no.: 098-0982934-2717: »Nature of the organic matter, interaction with traces and surfaces in the environment») and U.P. by the DFG (PA 424/6-2).

Figure captions

Fig.1. Square wave voltammograms showing A) Fe additions to a 0.5 mM BisTris solution in artificial seawater at pH 8 and B) scans of solutions of polysaccharides in artificial seawater at pH 8, 10-30 μ M Fe added, carrageenan shows specific sulphur peaks at -0.5 to -0.75 V.

Fig.2. CLE-CSV data of three polysaccharides titrated with iron, showing decreased sensitivity compared to UVSW, but no apparent stability constants could be derived.

Fig.3. The complexing capacity for Cu by *S.costatum* (1:5 diluted): A) Voltammograms of the Cu ions additions to 0.55M NaCl (additions of Cu ions are indicated). B) The data presented as concentrations of Cu ions added vs. Cu ion retrieved (measured). C) Results from B as free Cu ions retrieved vs. Cu ions retrieved/ complexed Cu ions.

Fig.4. A SWV voltammograms for A) *T.weissflogii* and B) *S.costatum* at pH =8.1 (solid line) and after acidification, purging with N₂ gas and readjustment the pH back to ~8.1 (dotted line). Experimental conditions: A) and B) Deposition potential, Ed = -0.2 V; deposition time td = 120 s; amplitude = 25 mV; frequency = 100 s⁻¹.

Fig.5. CPSA voltammogram of *S. costatum*. Experimental conditions: Potential of deposition, Ed = -0.2 V; constant current applied = 1 μ A; max.time of measurement = 5 s. Depositions time (t_d) are indicated in fig.

Fig.6. AC-voltammograms (potential vs. current curves) of phytoplankton cultures, phytagel (5mg/L) and a 0.55M NaCl solution. Experimental conditions: Potential of deposition, Ed = -0.6 V ; time of deposition, td = 60 s; amplitude = 10 mV.

Fig. 7. Concentrations of particulate and dissolved carbohydrates (= polysaccharide + monosaccharide), polysaccharides, monosaccharides, TEP, SAS and reduced sulfur species in phytagel (5mg/L) and in phytoplankton cultures of *S. costatum*, *T. weissflogii* and *E. huxleyi*).

Fig 1a

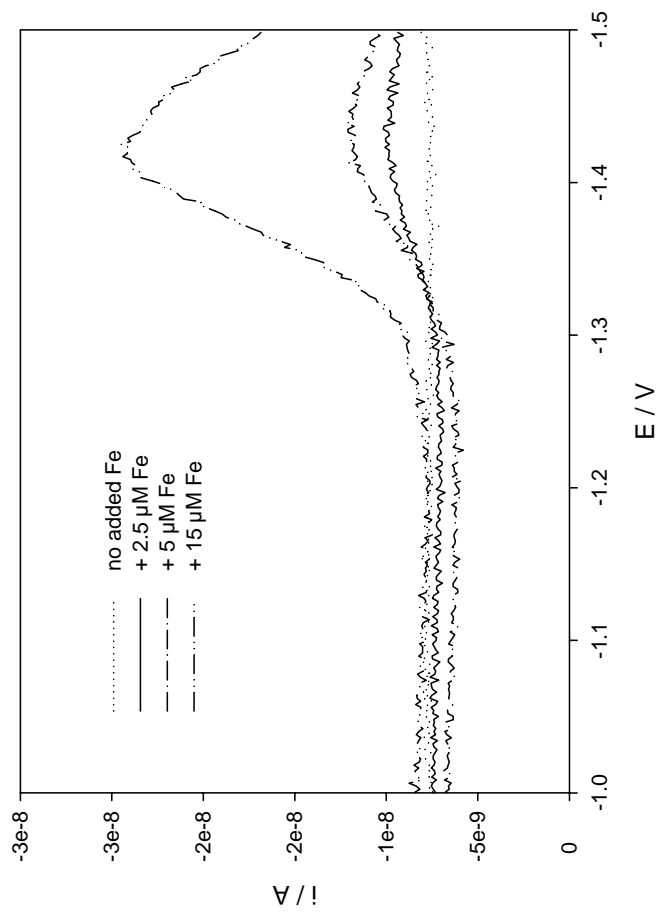
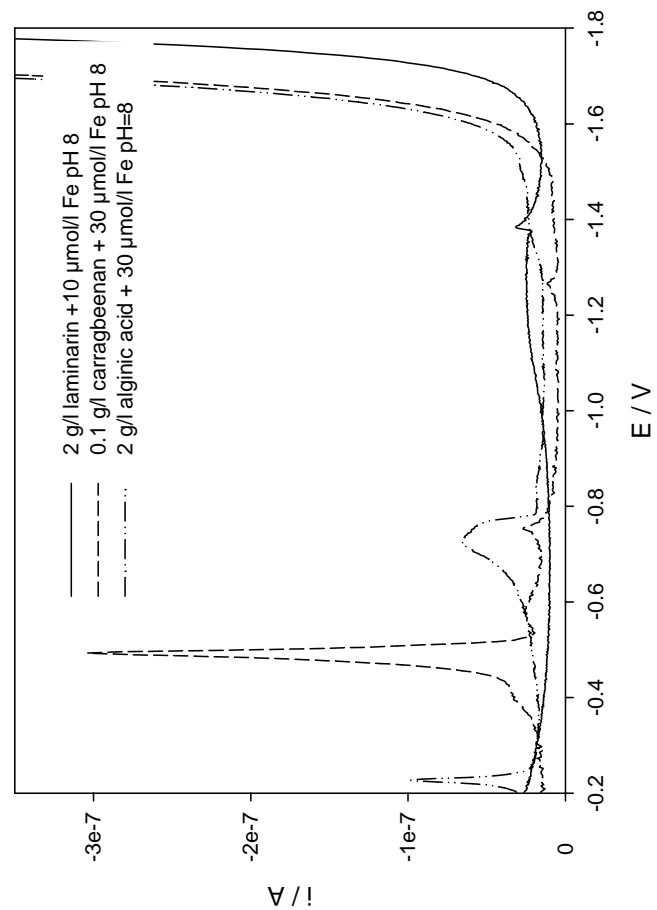


Fig 1b



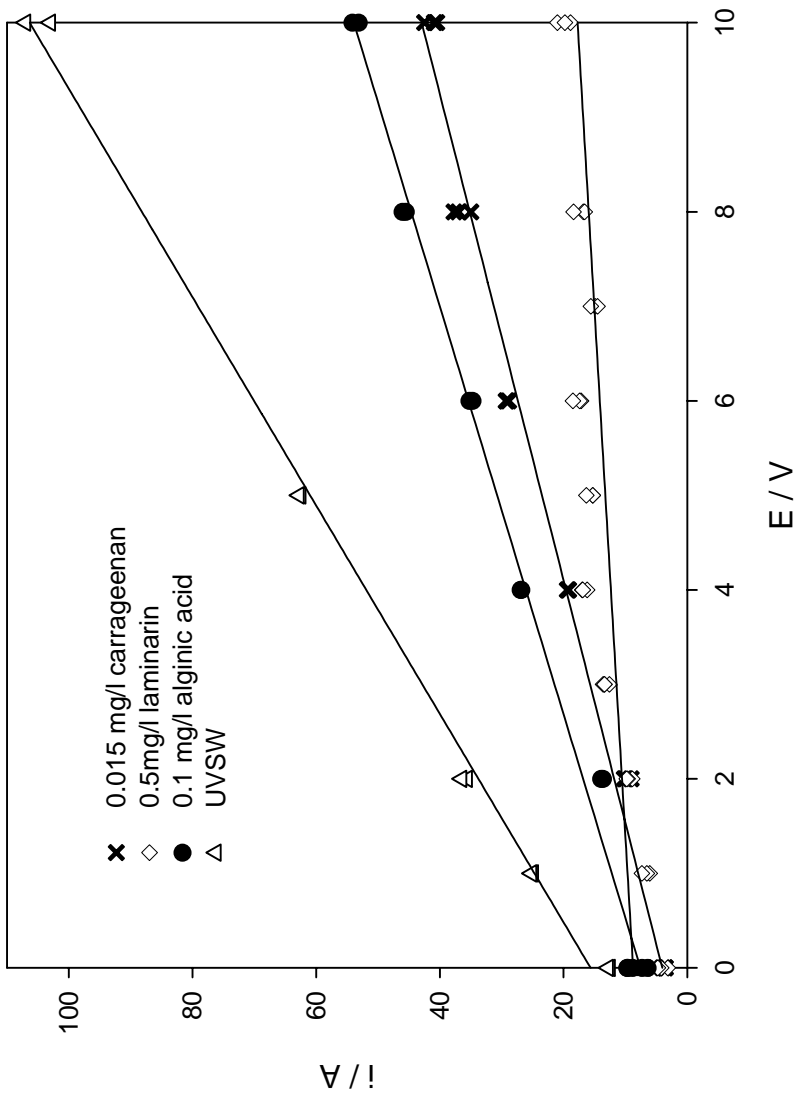
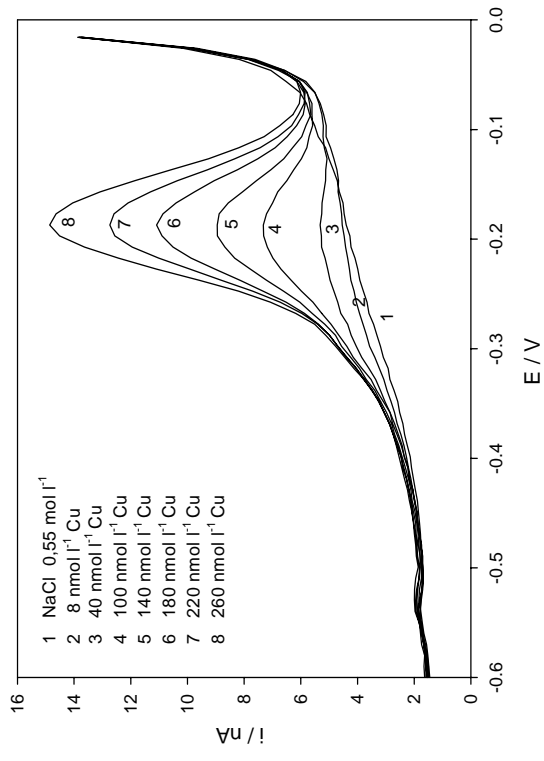
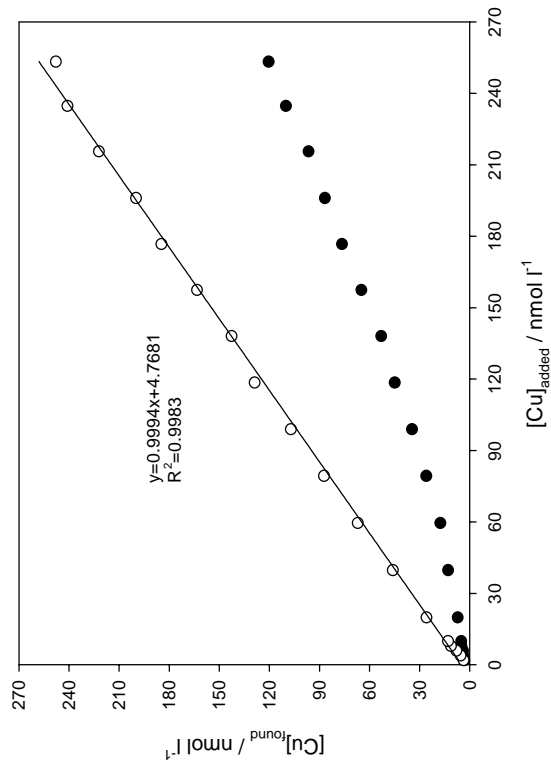
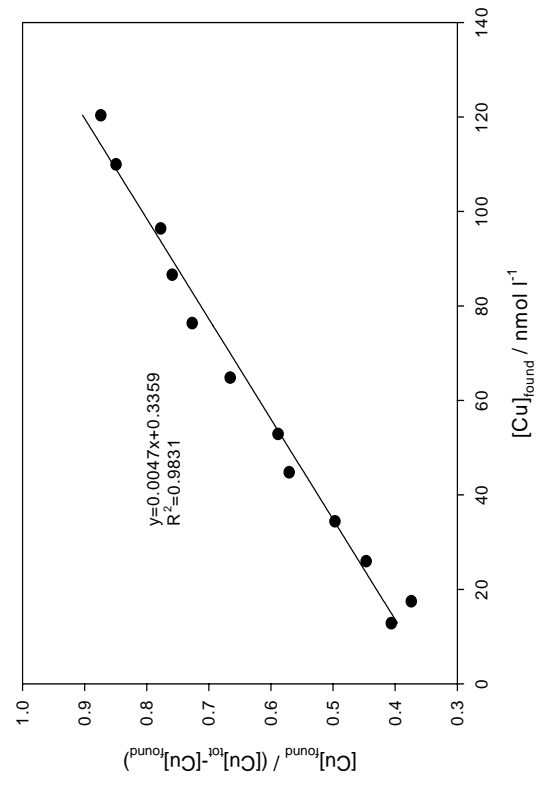


Fig 2

A**B****C****Fig 3**

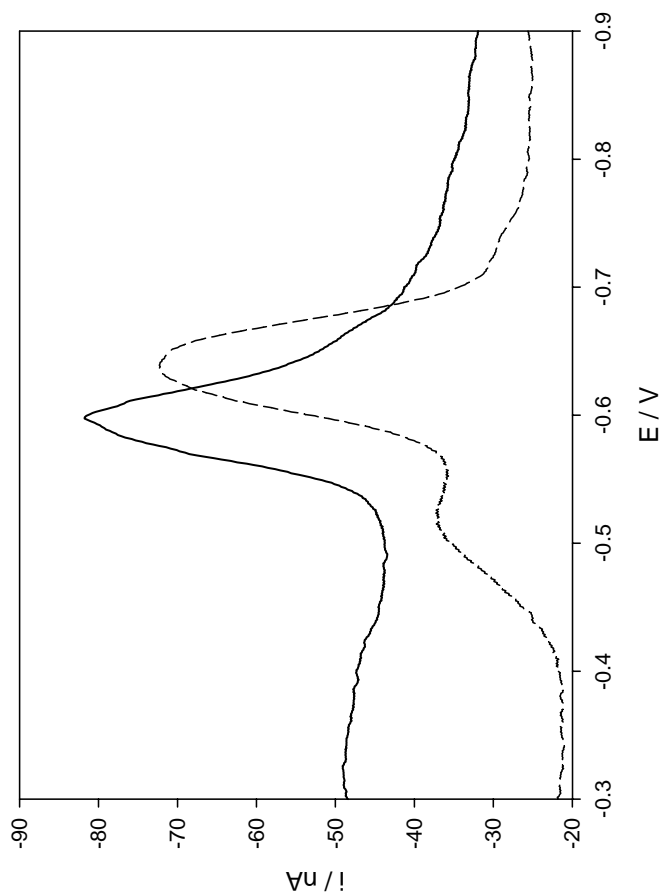


Fig 4b

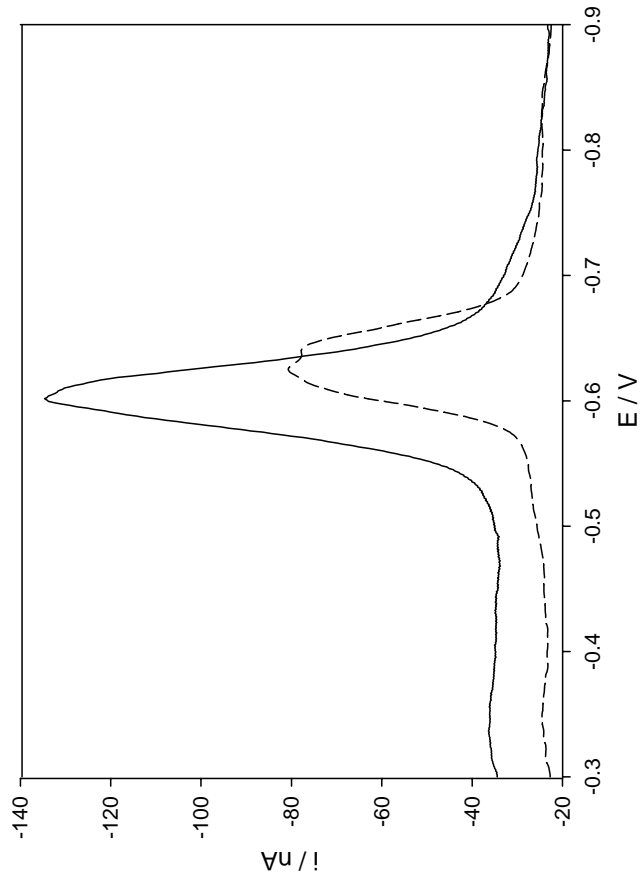


Fig 4a

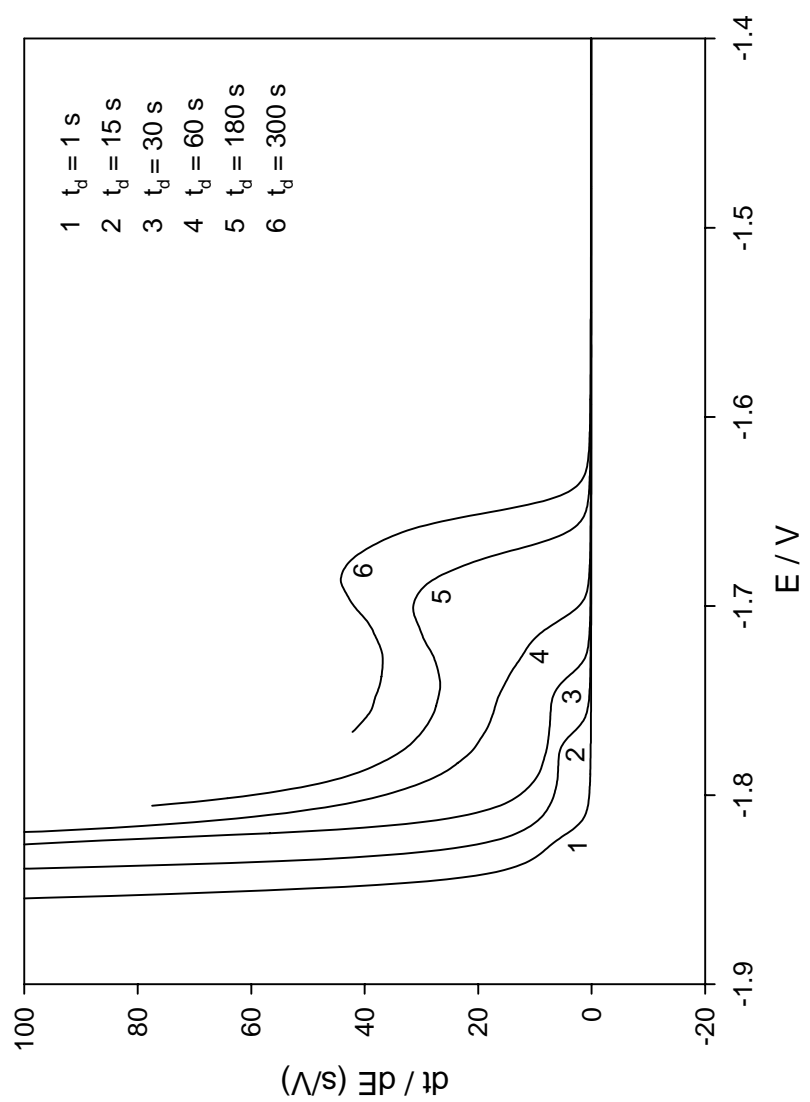
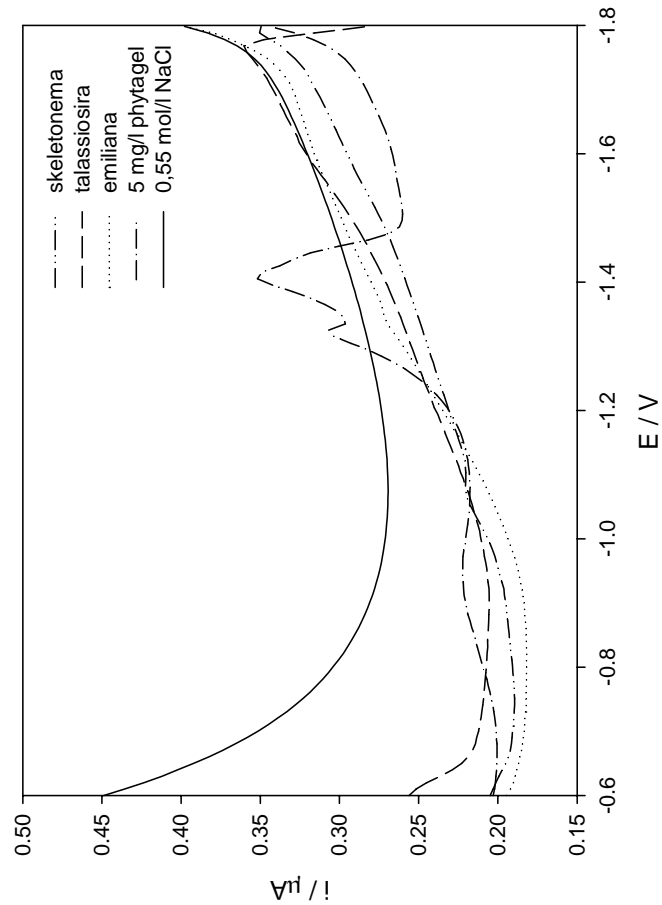


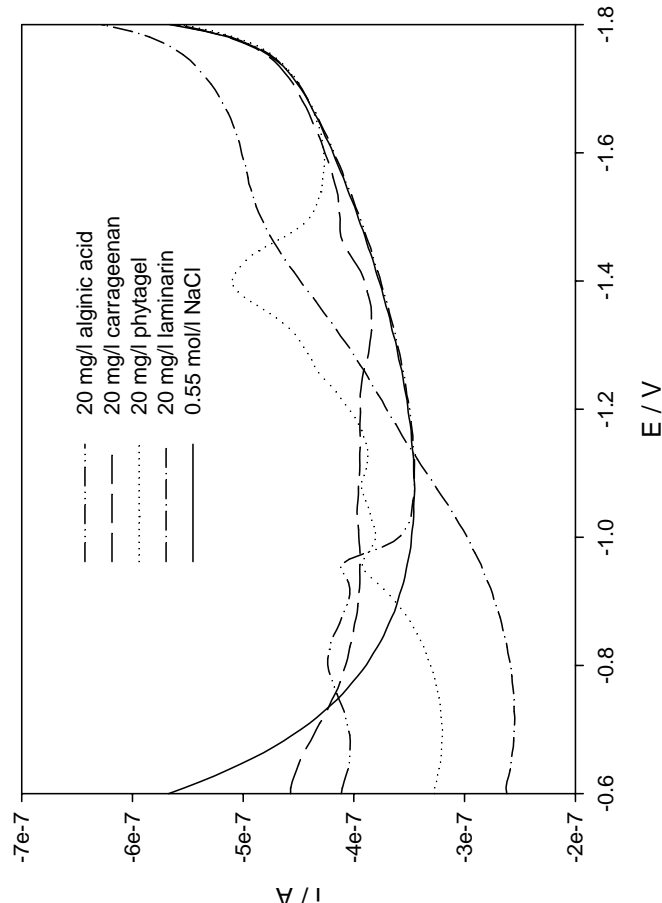
Fig 5

Fig 6

B



A



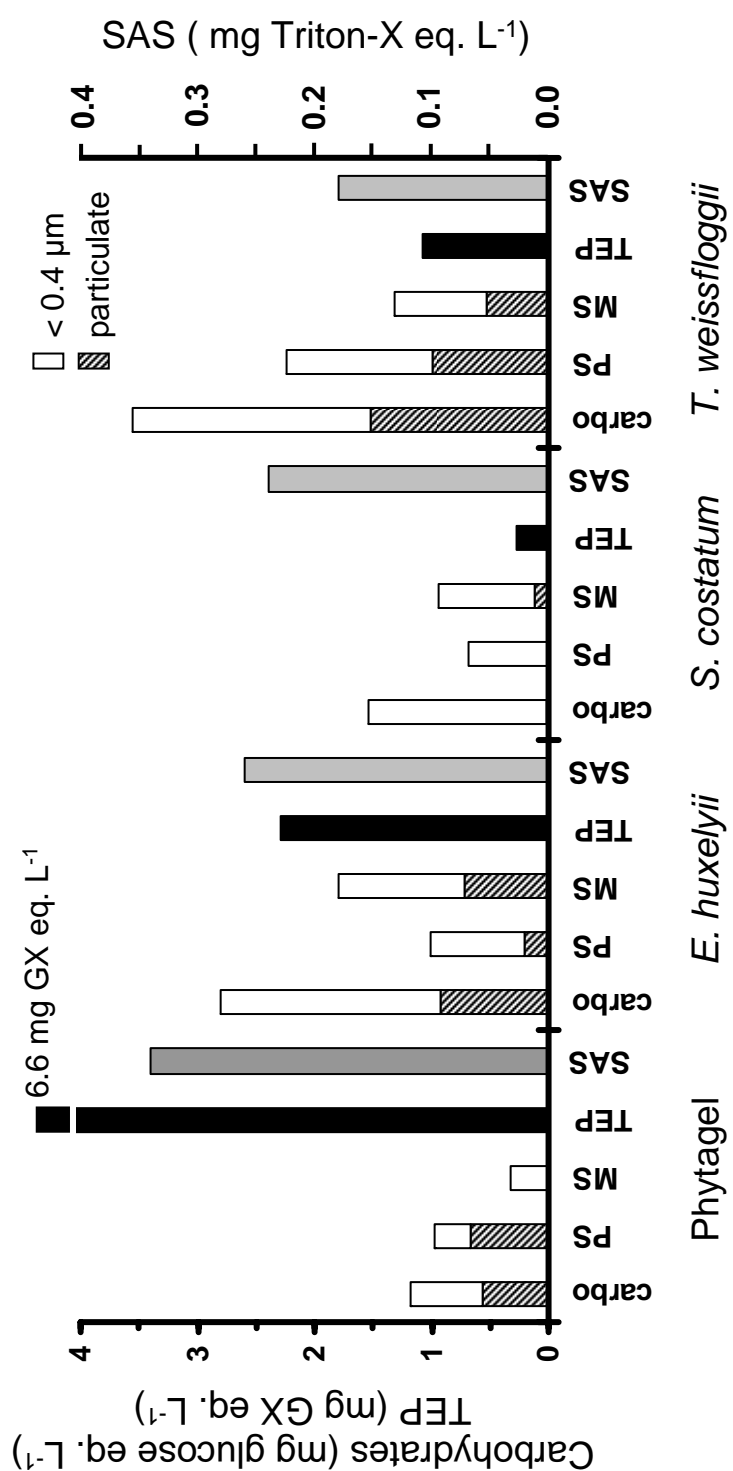


Fig 7

Table 1. Complexing properties and SAS in samples of the cultures of *Skeletonema costatum*, *Thalassiosira weissflogii*, *Emilia n huxleyi* and phytigel, a model substance.

Samples	Cu _T (nM)	CCu ¹ (μM)	Log K _{app Cu} ²	Cd _T (nM)	CCd ¹ (μM)	Log K _{app Cd} ²	SAS ³ (mg/L eq. Triton-X-100)	CPSA ⁴	Sulphur species(as eq. GSSG ⁵ nM)
<i>Skeletonema costatum</i>	23.80	1.06	6.45	16.45	0.022	8.73	0.24	yes	72
<i>Thalassiosira weissflogii</i>	26.60	1.14	6.18	14.85	0.020	8.83	0.18	no	200
<i>Emilia n huxleyi</i>	16.21	0.14	7.25	12.59	0.043	7.28	0.26	no	47
Phytigel (5 mg/L)	1.08	0.33	6.65	2.92	0.006	9.19	0.34	no	-
Phytigel (5 mg/L)	0.7 μm 0.2 μm	3.86 1.83	0.09 0.09	7.38 7.47	1.13 1.07	0.004 0.004	8.70 8.75	- 0.21	no no

¹Apparent complexing capacity for copper and cadmium ions; ²Apparent stability constant; ³Surface Active Substances; ⁴Constant current potentiometric stripping analysis-catalytic effect of NH₂ or/and SO₄²⁻ groups-appearance of the “pre”-sodium wave; ⁵glutathione; (-) not measured

CHAPTER 5:

Summary and conclusions

5 Summary and conclusions

Identifying the processes controlling the distribution of H₂O₂ in surface waters along a meridional transect in the Eastern Atlantic

In the present study H₂O₂ profiles were compared with physical and bio-optical measurements and available satellite data to determine the major processes controlling the distribution of H₂O₂ in the upper ocean along a meridional transect in the Eastern Atlantic. The measurements showed that a number of factors influenced H₂O₂ distribution. The latitudinal patterns observed identified irradiance, water temperature and recent precipitation as key controls. Vertical distributions of H₂O₂ were strongly controlled by its photoformation and mixing processes in the upper water column. The recent irradiation history and phytoplankton activity appear to be the major sources and sinks determining the observed H₂O₂ levels, with CDOM playing a minor role. This suggests sunlight is the key limiting reactant in the formation of H₂O₂ in the Tropical and Sub-Tropical surface ocean.

The role of polysaccharides and diatom exudates in the redox cycling of Fe and the photoproduction of hydrogen peroxide in coastal seawaters

In this study we investigated the photochemical effect of artificial and natural polysaccharide material in aquatic systems on iron speciation and production of H₂O₂. Artificial PS caused high photochemical production of H₂O₂, which on the one hand acts as a strong oxidant for metals and organic matter and on the other hand, is formed photochemically via the superoxide intermediate which is capable of reducing Fe(III). Increased steady state Fe(II) concentrations were found in illuminated seawater with high concentrations of exudates of *Phaeodactylum tricornutum*. In the dark, this effect of artificial PS on ferrous iron was not detectable suggesting that light-produced

superoxide reduces Fe(III), maintaining elevated Fe(II) concentration. In coastal seawater with high content of organic matter originating partly from diatoms, a positive effect of the exudates on the bioavailability of iron seems likely.

Characterization of phytoplankton exudates and polysaccharides in relation to their complexing capacity of copper, cadmium and iron

The goals of this study were to determine electrochemically, the complexing capacity of organic matter released by cultures of two marine diatoms *Thalassiosira weissflogii* and *Skeletonema costatum*, as well as the coccolithophore *Emiliania huxleyi* to copper (CCu) and cadmium (CCd) as well as to determine the organic matter responsible for the complexation. In particular, the constituents of organic matter whose effects were investigated were reduced sulphur species (RSS), of surface active substances (SAS), thio/amino groups, transparent exopolymer particles (TEP) and carbohydrates.

Phytagel, carrageenan, laminarin and alginic acid were analysed as model substances.

The organic matter released by all three phytoplankton cultures and the polysaccharide phytagel complexed Cu and to a lesser extent Cd. However, Cd complexes showed higher apparent stability constants and consequently the exudates and phytagel bound Cd more specifically than Cu. Sulphur-rich “glutathione” type ligands were found in all phytoplankton samples and were possibly responsible for the complexation of Cu. The correlation of monosaccharides with the complexing capacity to Cd, indicated that in the phytoplankton samples these compounds bound Cd. TEP, SAS and polysaccharides did not appear to be responsible for the complexing properties of the phytoplankton and no specific iron binding properties of laminarin, carrageenan and alginic acid could be found, probably partly due to limitations of the applied electrochemical methods. However, these measurements confirmed that the analysed model polysaccharides are highly surface active.

Conclusions

The findings of the experimental work confirmed hypothesis 1.1 “Algal exudates stabilise Fe(II)”, but only under UV irradiation, probably due to reduction of Fe by superoxide. Hypothesis 1.2 “Fe bound to polysaccharides is released via photochemical processes” could not be confirmed, as it appeared that polysaccharides did not bind iron. Despite that, the photochemical production of H₂O₂ via the superoxide radical, which presumably reduced Fe, was enhanced in the presence of polysaccharides and diatom exudates, respectively.

The in situ measurements of H₂O₂ along a meridional transect in the Eastern Atlantic partly confirmed hypothesis 2 “Phytoplankton exudates enhance the photoproduction of H₂O₂, a major player in the redox chemistry of Fe”, as the vertical distributions of H₂O₂ were controlled by phytoplankton activity, but the correlations with CDOM were poor.

Hypothesis 3. “Acidic polysaccharides and TEP are strong Fe chelators contributing significantly to the pool of unknown organic Fe-ligands in the ocean, released by diatoms to prevent Fe from precipitating from the surface ocean” could not be confirmed and no specific Fe complexation was found. Nevertheless, methodological limitations seemed to have obstructed a satisfactory conclusion.

CHAPTER 6:

Future work

6 Future work

This three year project gave significant new insights into the effect of polysaccharides and diatom exudates on the photochemical H₂O₂ formation and on the Fe(II) oxidation kinetics as well as the widely assumed potential contribution of these compounds to the pool of Fe ligands. As a result, this work has deepened our knowledge of iron biogeochemistry in the marine environment. Nevertheless, it is necessary to extend this work to draw further conclusions about this topical subject.

6.1 The role of polysaccharides and diatom exudates in the redox cycling of Fe and the photoproduction of hydrogen peroxide in coastal seawaters

In order to extend the laboratory results of this study to natural environments which have at least 100 times lower total iron concentrations, measurements over a range of pH, ligand concentrations, iron concentrations, and light fluxes have to be made. These data will also provide the mechanistic details for a more advanced modeling of Fe(III) speciation, the influence of Fe(II) oxidation on H₂O₂ reduction, the influence of superoxide concentrations on Fe(III) and Fe(II) redox kinetics and changes in Fe(II) oxidation stoichiometry as a function of total iron concentration. This will be a valuable contribution to our mechanistic understanding of the redox chemistry of iron in seawater. Furthermore, in situ measurements of photoproduction of H₂O₂, TEP and polysaccharide concentrations, iron speciation and lifetime of Fe(II) in presence of natural phytoplankton exudates during bloom events will help to estimate the importance of polysaccharides and diatom exudates in the redox cycling of Fe.

6.2 Identifying the processes controlling the distribution of H₂O₂ in surface waters along a meridional transect in the Eastern Atlantic

To get a broader picture of the H₂O₂ distribution on a global scale, more surveys in different oceanic regions and at different times in the year are needed. Parallel monitoring of biological, chemical and physical parameters like chl. a, TEP/PS and CDOM, water temperature and irradiance will reveal the processes controlling global H₂O₂ distributions. This could lead to the development of parameterization schemes for the prediction of H₂O₂ distribution from satellite data, which would be an invaluable contribution to the modelling of the marine Fe biogeochemistry.

6.3 Characterization of phytoplankton exudates and polysaccharides in relation to their complexing capacity of copper, cadmium and iron

The results of this study were affected by limitations of the electrochemical method. The necessary high iron concentrations enhanced the hydrolysis which affected the sensitivity and reproducibility of the measurements. The high surface activity of the polysaccharides also led to a decreased sensitivity which made satisfactory results difficult. The detection limit of this method also seemed to be too high.

A different reasonable approach could aim to determine the bioavailability of iron in presence of polysaccharides and phytoplankton exudates. This can be done by means of growth and uptake experiments with radioactive ⁵⁵Fe in natural phytoplankton populations.

Room for more research remains!

CHAPTER 7:

References

7 References

- Aluwihare, L., D. Repeta, *et al.* (1997). "A major biopolymeric component of dissolved organic carbon in surface sea water." *Nature* **387**: 166-169.
- Aluwihare, L. I. and D. J. Repeta (1999). "A comparison of the chemical characteristics of oceanic DOM and extracellular DOM produced by marine algae." *Mar. Ecol. Prog. Ser.* **186**: 105-117.
- Barbeau, K., J. W. Moffett, *et al.* (1996). "Role of protozoan grazing in relieving iron limitation of phytoplankton." *Nature* **380**: 61-64.
- Benner, R. (2002). Chemical composition and reactivity. *Biogeochemistry of dissolved organic matter*. D. A. Hansell and C. Carlson. New York, Academic Press, Elsevier Science: 59-90.
- Boyd, P. W., T. Jickells, *et al.* (2007). "Mesoscale iron enrichment experiments 1993–2005: synthesis and future directions." *Science* **315**: 612-617.
- Boye, M. (2001). "Organic complexation of iron in the Southern Ocean." *Deep Sea Research I* **48**(6): 1477-1497.
- Bruland, K. W., J. R. Donat, *et al.* (1991). "Interactive influence of bioactive tracemetals on biological production in oceanic waters." *Limnol. Oceanogr.* **36**: 1555-1577.
- Butler, A. (2005). "Marine siderophores and microbial iron mobilization." *Biometals* **18**(4): 369-374.
- Coale, K. (1991). "Effects of iron, manganese, copper and zinc enrichments on the productivity and biomass in the subarctic Pacific." *Limnol. Oceanogr.* **36**: 1851-1864.
- Cooper, W. J., R. G. Zika, *et al.* (1988). "Photochemical formation of H₂O₂ in natural waters exposed to sunlight." *Environ. Sci. Technol.* **22**: 1156-1160.
- Croot, P. L. and M. Johansson (2000). "Determination of iron speciation by cathodic stripping voltammetry in seawater using the competing ligand 2-(2-Thiazolylazo)-p-cresol (TAC)." *Electroanalysis* **12**(8): 565-576.
- Croot, P. L., B. Karlson, *et al.* (1999). "Uptake of 64Cu-Oxine by Marine Phytoplankton." *Environmental Science and Technology* **33**(20): 3615-3621.
- Croot, P. L., P. Laan, *et al.* (2005). "Spatial and temporal distribution of Fe(II) and H₂O₂ during EisenEx, an open ocean mesoscale iron enrichment." *Mar. Chem.* **95**: 65-88.
- De Baar, H. J. W. and P. W. Boyd (2000). The role of iron in plankton ecology and carbon dioxide transfer of the global oceans. *The dynamic ocean carbon cycle: a midterm synthesis of the joint global ocean flux study. International geosphere biosphere programme book series*. R. B. Hanson, H. W. Ducklow and G. S. Field. Cambridge, Cambridge University Press. **5**: 61-140.

Falkowski, P. G., R. T. Barber, *et al.* (1998). "Biogeochemical controls and feedbacks on ocean primary production." Science **281**(5374): 200-206.

Geider, R.J, *et al.* (1994). "The role of iron in phytoplankton photosynthesis and the potential for iron-limitation of primary productivity in the sea." Photosynth. Res. **39**: 275-301.

Geider, R. J. (1999). "Complex lessons if iron uptake." Nature **400**: 815-816.

Gledhill, M. (2007). "The determination of heme b in marine phyto- and bacterioplankton." Mar. Chem. **103**(3-4): 393-403.

Guo, L., P. H. Santschi, *et al.* (2002). "Metal partitioning between colloidal and dissolved phases and its relation with bioavailability to American oysters." Marine Environmental Research **54**(1): 49-64.

Hutchins, D. A. and K. W. Bruland (1994). "Grazer mediated regeneration and assimilation of Fe, Zn and Mn from planctonic prey." Mar. Ecol. Prog. Ser. **110**: 259-269.

Hutchins, D. A., A. E. Witter, *et al.* (1999). "Competition among marine phytoplankton for different chelated iron species." Nature **400**: 858-861.

King, D. W., H. A. Lounsbury, *et al.* (1995). "Rates and mechanism of Fe(II) oxidation at nanomolar total iron concentrations." Environ. Sci. Technol. **29**: 818-824.

Macrellis, H. M., C. G. Trick, *et al.* (2001). "Collection and detection of natural iron-binding ligands from seawater." Marine Chemistry **76**: 175-187.

Maldonado, M.T, *et al.* (1999). "Utilization of iron bound to strong organic ligands by plankton communities in the subarctic Pacific Ocean." Deep-Sea Res. II **46**(11-12): 2447-2473.

Martin and J.H (1990). "Glacial-interglacial CO₂ change: The iron hypothesis." Paleoceanography **5**: 1-13.

Martin, J.H, *et al.* (1988). "Iron deficiency limits phytoplankton growth in the northeast Pacific subarctic." Nature **331**: 341-343.

Miles, C. J. and P. L. Brezonik (1981). "Oxygen consumption in humic-colored waters by a photochemical ferrous-ferric catalytic cycle." Environ. Sci. Technol. **15**(9): 1089-1095.

Millero, F. J. and S. Sotolongo (1989). "The oxidation of Fe(II) with H₂O₂ in seawater." Geochim. Cosmochim. Acta **53**: 1867-1873.

Millero, F. J., S. Sotolongo, *et al.* (1987). "The oxidation kinetics of Fe(II) in seawater." Geochim. Cosmochim. Acta **51**: 793-801.

Mopper, K., J. Zhou, *et al.* (1995). "The role of surface-active carbohydrates in the flocculation of a diatom bloom in a mesocosm." Deep Sea Research II **42**: 47-73.

Morel, F. M. M. and N. M. Price (2003). "The biogeochemical cycles of trace metals in the

oceans." *Science* **300**: 944-947.

Nakabayashi, S., K. Kuma, *et al.* (2002). "Variation in iron(III) solubility and iron concentration in the northwestern North Pacific Ocean." *Limnology and Oceanography* **47**(3): 885-892.

Nolting, R. F., L. J. A. Gerringa, *et al.* (1998). "Fe(III) speciation in the high nutrient low chlorophyll Pacific region of the Southern Ocean." *Mar. Chem.* **62**: 335-352.

Quigley, M. S., P. H. Santschi, *et al.* (2001). "Sorption irreversibility and coagulation behavior of ^{234}Th with marine organic matter." *Mar. Chem.* **76**: 27-45.

Quigley, M. S., P. H. Santschi, *et al.* (2002). "Importance of acid polysaccharides for ^{234}Th complexation to marine organic matter." *Limnol. Oceanogr.* **47**: 367-377.

Rose, A. L. and T. D. Waite (2002). "Kinetic model for Fe(II) oxidation in seawater in the absence and presence of natural organic matter." *Environ. Sci. Technol.* **36**: 433-444.

Rose, A. L. and T. D. Waite (2003). "Effect of Dissolved Natural Organic Matter on the Kinetics of Ferrous Iron Oxygenation in Seawater." *Environ. Sci. Technol.* **37**: 4877-4886.

Rue, E. L. and K. W. Bruland (1995). "Complexation of iron(III) by natural organic ligands in the central North Pacific as determined by a new competitive ligand equilibrium / adsorptive cathodic stripping voltammetric method." *Marine Chemistry* **50**: 117-138.

Santschi, P. H. (1997). "Colloids in oceanic environments: Composition and importance for trace element cycles." *Abstracts of Papers American Chemical Society* **214**(1-2).

Scully, N. M., D. J. McQueen, *et al.* (1996). "Hydrogen peroxide formation: The interaction of ultraviolet radiation and dissolved organic carbon in lake waters along a 43-75 degrees N gradient." *Limnol. Oceanogr.* **41**(3): 540-548.

Sedlak, D. L. and J. Hoigne (1993). "The role of copper and oxalate in the redox cycling of iron in atmospheric waters." *Atmospheric Environment* **27A**(14): 2173-2185.

Sunda, W. G. and S. A. Huntsman (1995). "Cobalt and zinc interreplacement in marine phytoplankton: Biological and geochemical implications." *Limnol. Oceanogr.* **40**(8): 1404-1417.

Theis, T. L. and P. C. Singer (1974). "Complexation of Iron(II) by organic matter and its effect on Iron(II) oxygenation." *Environ. Sci. Technol.* **8**: 569-573.

van den Berg, C. M. G. (1995). "Evidence for organic complexation of iron in seawater." *Marine Chemistry* **50**: 139-157.

Waite, T. D. and F. M. M. Morel (1984). "Photoreductive dissolution of colloidal iron oxides in natural waters." *Environmental Science & Technology* **18**: 860-868.

Wells, M. L. and E. D. Goldberg (1993). "Colloid aggregation in seawater." *Mar. Chem.* **41**: 353-358.

Wilhelm, S. W. and C. G. Trick (1994). "iron-limited growth of cyanobacteria: Multiple siderophore production is a common response." Limnology and Oceanography **39**(8): 1997-1984.

Yocis, B. H., D. J. Kieber, *et al.* (2000). "Photochemical production of hydrogen peroxide in Antarctic Waters." Deep Sea Research I **47**(6): 1077-1099.

Yuan, J. and A. M. Shiller (2001). "The distribution of hydrogen peroxide in the southern and central Atlantic ocean." Deep Sea Research II **48**: 2947-2970.